Status of Computational Aerodynamic Modeling Tools for Aircraft Loss-of-Control

Neal T. Frink[1], Patrick C. Murphy[2], Harold L. Atkins[3], Sally A. Viken[4], and Justin L. Petrilli[5]
NASA Langley Research Center, Hampton, VA, 23681

Ashok Gopalarathnam[6] and Ryan C. Paul[7]
North Carolina State University, Raleigh, North Carolina, 27695

A concerted effort has been underway over the past several years to evolve computational capabilities for modeling aircraft loss-of-control under the NASA Aviation Safety Program. A principal goal has been to develop reliable computational tools for predicting and analyzing the non-linear stability & control characteristics of aircraft near stall boundaries affecting safe flight, and for utilizing those predictions for creating augmented flight simulation models that improve pilot training. Pursuing such an ambitious task with limited resources required the forging of close collaborative relationships with a diverse body of computational aerodynamicists and flight simulation experts to leverage their respective research efforts into the creation of NASA tools to meet this goal. Considerable progress has been made and work remains to be done. This paper summarizes the status of the NASA effort to establish computational capabilities for modeling aircraft loss-of-control and offers recommendations for future work.

Nomenclature

C_l, C_L	=	sectional lift coefficient, total lift coefficient
C_m	=	pitching moment coefficient about y-body axis
C_n	=	yawing moment coefficient about z-body axis
C_{n_β}	=	yaw stability derivative, $\Delta C_n/\Delta\beta$ at $\beta=0°$
C_N	=	normal force coefficient
C_p	=	pressure coefficient
mac, m.a.c.	=	mean aerodynamic chord
M	=	freestream Mach numb
Re_{cref}	=	Reynolds number based on reference chord
α	=	angle-of-attack, deg.
β	=	angle-of-sideslip, deg. Positive nose left (wind from right)
$\Delta\alpha$	=	incremental step change in angle-of-attack, deg

Key Acronyms

AFM	=	Advancing Front Method
ALM	=	Advancing Layers Method
ATD	=	Airspace Technology Demonstrations Program
AvSafe	=	NASA Aviation Safety Program
AVT	=	Applied Vehicle Technology

[1] Senior Research Engineer, Configuration Aerodynamics Branch, MS 499, AIAA Associate Fellow
[2] Senior Research Engineer, Dynamic Systems & Control Branch, MS 308, AIAA Associate Fellow
[3] Senior Research Scientist, Computational AeroSciences Branch, MS 128
[4] Assistant Branch Head for Configuration Aerodynamics Branch, MS 499, AIAA Senior Member
[5] Research Engineer, Flight Dynamics Branch, MS 308
[6] Associate Professor, Box 7910, ashok g@ncsu.edu, (919) 515-5669. Associate Fellow, AIAA
[7] Graduate Research Assistant, Box 7910, rcpaul@ncsu.edu. Student Member, AIAA

CFD	=	Computational Fluid Dynamics
FAA	=	Federal Aviation Administration
GTM	=	Generic Transport Model
HT	=	Horizontal tail
IRAC	=	Integrated Resilient Aircraft Control project
LaRC	=	Langley Research Center
LOC	=	Loss of control
RANS	=	Reynolds Averaged Navier Stokes
ROM	=	Reduced order model
SA	=	Spalart-Allmaras one equation turbulence model
SACCON	=	Stability and Control Configuration
SID	=	System Identification
SST	=	Menter's Shear Stress Transport two equation turbulence model
STO	=	NATO Science and Technology Organization
TASEAS	=	Technologies for Assuring Safe Aircraft Energy and Attitude State project
UCAV	=	Unmanned combat air vehicle
VLM	=	Vortex Lattice Method
VSST	=	Vehicle Systems Safety Technologies project
VT	=	Vertical tail
WT	=	Wind Tunnel
12FT LWT	=	NASA LaRC 12 Foot Low Speed Tunnel
14X22	=	NASA LaRC 14X22 Foot Subsonic Tunnel

I. Introduction

NASA has been engaged in long-term research under the Aviation Safety (AvSafe) program[1] to improve the safety of commercial transport aircraft. This research spans a broad scope from multiple systems down through fundamental physics and modeling. Flight safety depends on a complex interaction of integrated systems and is ultimately a matter of maintaining airworthiness and control in the event of onboard system failure, airframe damage, icing, or extreme upset. The goal of the Aviation Safety Program was to identify and develop tools, methods, and technologies for improving overall aircraft safety of new and legacy vehicles operating in the Next Generation Air Transportation System. The objectives of the program were to conduct cutting-edge research that will produce tools, methods, concepts and technologies to improve the intrinsic safety attributes of current and future aircraft and overcome safety barriers that could otherwise constrain the full realization of NextGen.

Loss-of-control (LOC) remains one of the largest contributors to fatal aircraft accidents [1]. The causes of aircraft loss-of-control can range from a complex sequence of events that result in vehicle upset, to a more straightforward physical degradation of the airframe from damage or icing. While there is no single intervention strategy, the outcome will often depend on a timely response from the pilot and/or onboard flight control system to restore safe flight, or a rapid reconfiguration of the flight controls to compensate for airframe degradation. Of course, the best LOC intervention strategy is through prevention by understanding and mitigating the factors leading up to a potentially catastrophic event. NASA has been addressing these challenges for the past decade. In the process, a large body of wind tunnel data [2] to [8] has been developed to quantify the static and dynamic aerodynamics and stability & control (S&C) characteristics on a conventional subsonic transport due to 1) damage to lifting, stability, and control surfaces, 2) icing deformation, and 3) extreme post-stall flight upset conditions. These data comprise a unique foundation for deciphering the conflicting aerodynamic factors that lead to aircraft loss-of-control.

The Federal Aviation Administration (FAA) has added a new requirement RIN-2120-AJ00 [9] that enhanced flight simulator models to be implemented by early 2019 for training pilots to recognize precursors to stall and to learn upset recovery strategies. Many of the fatal accidents to date have resulted from incorrect pilot responses because of disorientation and heavy reliance on automation [1]. The technical challenge arises from how to construct augmented LOC reduced-order models (ROM) to meet the new LOC training requirement. One must first know the level of modeling needed to create sufficient representations of aircraft stall and post stall behavior for training purposes. For example, is it sufficient to create a generic stall model for civil transports that can be augmented to reflect configuration-specific stall behavior? The answers to these questions are being sought through various studies, [10] to [13].

[1] http://www.aeronautics.nasa.gov/programs_avsafe.htm

Flight simulator ROM's are typically constructed using an array of data from wind tunnel tests, and full-scale flight data. For practical reasons, simulation models typically assume aerodynamic coefficients can be expressed in series expansions thus creating the commonly used stability and control derivatives. In wind tunnels, conventional practice to obtain damping derivatives is accomplished by measuring the in-phase and out-of-phase responses from forced oscillations on wind-tunnel models. Such measurements are typically obtained at very low-speeds, which severely limit the data to very low Reynolds and Mach numbers, and because of test rig kinematic constraints only coupled derivatives can be measured. These limitations result in simplifications to the models and restrict application to normal and benign regions of the flight envelope. These models do not capture unsteady responses and only limited nonlinearity is accommodated. Promising research is also underway at NASA Langley Research Center in computational, ground-based, and flight-test methods to extend models beyond these limitations. Research in flight-test methods using a subscale flight model called AirStar to develop techniques for real-time extraction of stability and control derivatives from both subscale and full-scale air vehicles is summarized in Refs. [14] to [17]. Research in wind-tunnel test methods and early efforts to apply those methods to CFD simulation results are highlighted in section VIII-B.

With the advent of computational aerodynamic analysis tools, computational fluid dynamics (CFD) offers another source of data to create configuration-specific ROMs for stall scenarios. Such technology opens new options beyond what is physically possible in wind-tunnel or subscale flight experiments. For example, the CFD model can be "flown" through maneuvers that are not physically possible using experimental techniques, such as indicial maneuvers that isolate angular and rate terms for creating decoupled dynamic derivatives [18]. Furthermore, CFD can generate vehicle-specific dynamic derivatives across the full flight Reynolds and Mach number range.

II. AvSafe CFD Strategy

A. Goals and objectives

The CFD Loss-of-Control work has been sponsored under the NASA AvSafe program, Integrated Resilient Aircraft Control (IRAC) project from 2008-2010 and Vehicle Systems Safety Technologies (VSST) project from 2011-2014, and the Airspace Operations and Safety Program, Airspace Technology Demonstrations (ATD) project from late 2014 to the present. Within the ATD project, the CFD Loss-of-Control work has been conducted in the Technologies for Assuring Safe Aircraft Energy and Attitude State (TASEAS) work element. One of the common technical challenges consistently addressed across the projects is to maintain safe and effective aircraft control around the stall boundaries. At such conditions, the aircraft experiences highly non-linear static/dynamic aerodynamic behavior. The following describes an approach devised to guide a small investigative team in exploring the applicability of CFD methods for addressing these challenges.

1. CFD plan 2008-2011

The initial CFD plan was devised around the goal to "Develop reliable computational tools for predicting and analyzing stability and control characteristics of aircraft in damage, icing, and upset flight conditions". A two-track approach was pursued to 1) perform CFD code calibration studies of static and dynamic aerodynamics for the Generic Transport Model (GTM) shown in **Figure 1** with and without airframe damage, while 2) simultaneously researching the issues and feasibility of applying System Identification (SID) techniques to CFD data for creating non-linear ROMs that can be used in flight simulators. Multi-code CFD calibration studies were conducted for the static and dynamic aerodynamic characteristics of the GTM across a broad range of angle-of-attack and sideslip, followed by investigations of the impact of airframe degradations, such as damage and icing. The icing studies were encouraged through communications with personnel at NASA Glenn Research Center. A stretch goal was included to investigate control surface effects, but was not addressed due to resource limitations. In parallel with the CFD calibration work, collaboration was coordinated with the NASA LaRC Dynamic Systems and Control Branch to assess the issues and feasibility of applying SID techniques to CFD data for augmenting flight simulation models. Hence, these investigations serve as a foundation for advancing the ultimate goal of augmenting flight simulator models with more realistic aerodynamic data for airframe damage, icing, and flight upset scenarios.

2. CFD plan 2012 to present

In late 2011, the CFD plan was revised to have more focus on capturing the dynamic S&C characteristics of aircraft LOC, and to insert them into the system identification process for creating improved ROMs. The stated goal was revised to "Develop reliable computational tools for predicting and analyzing the non-linear stability & control characteristics of aircraft near the stall boundaries affecting safe flight, and for utilizing those predictions for creating augmented flight SIM models that improve pilot training for adverse flight scenarios". The new plan was formulated with more direct coordination between the CFD dynamic S&C modeling work and the system identification flight simulation modeling efforts.

B. Key external collaboration

A key external collaboration was cultivated through the first author's participation in three North Atlantic Treaty Organization (NATO) Science and Technology Organization (STO) Applied Vehicle Technology (AVT) task groups. From 2007-2010, the first task group AVT-161 titled "Assessment of Stability and Control Prediction Methods for NATO Air & Sea Vehicles" assessed the state-of-the-art in CFD methods for the prediction of static and dynamic stability and control characteristics of military vehicles in the air and sea domains. The air facet focused a generic 53° swept unmanned combat air vehicle (UCAV) configuration called the Stability and Control Configuration (SACCON) [19]. The AVT-161 team was composed of 46 researchers from 14 countries using 7 CFD codes that published a Final Report of 26 chapters, summarized in Refs. [19], [20], 8 journal articles [21] to [28], and 27 workshop papers presented in a Specialist Meeting (AVT-189) and summarized in Refs. [29] and [30]. This documentation provides a comprehensive record of the state-of-the-art of S&C prediction on the highly nonlinear flow field of SACCON and sea vehicles. In the four years that AVT-161 team existed, it is estimated that the participating nations spent over €10 million on building and testing both wind-tunnel and water-tank models, to compile a database of experimental results, while running large computer models to produce analytical data comparisons. This evolving knowledge was continually infused into the AvSafe VSST project by maintaining parallel S&C studies on the GTM configuration.

Participation continued with a follow-on AVT-201 task group titled "Extended Assessment of Reliable Stability & Control Prediction Methods for NATO Air Vehicles" (2012-2015) [31]. Some of the primary goals of this group are to 1) investigate techniques for creating flight simulation models from CFD predictions, 2) build S&C data bases from experimental and CFD predictions to compare impact on flight simulation accuracy, and 3) determine level of accuracy and sensitivity of flight simulation using CFD when compared with models built from experimental data. The AVT-201 team, comprised of 35 researchers from 9 countries using 7 CFD codes, is charged with exploring a range of strategies for creating CFD-derived simulation models across the highly non-linear flight envelope (such as "flying" multi-spectrum model estimation maneuvers, reduced-order modeling or combined low-fidelity/high-fidelity approaches, etc.). The team is currently active and in the process of writing the Final Report and journal articles. As with the preceding task group, the ideas and technologies from AVT-201 for creating nonlinear ROMs from CFD are being assessed for application to the Airspace Operations and Systems program for civil transports [32].

Because the prediction of flow separation during stall is highly dependent on turbulence models, the first author was also involved in the AVT-183 task group titled "Reliable Prediction of Separated Flow Onset and Progression for Air and Sea Vehicles" (2010-2014). The goal of this task group was to provide data and understanding that might lead to improvements in turbulence models that result in more accurate predictions of round leading-edge flow separation. The focus configuration was a 53° swept-diamond wing with round leading edge [33], [34]. Hence, most derived benefits to NASA would apply to future vehicle concepts, such as a Hybrid Wing Body and supersonic business jets.

III. Computational data requirements for LOC

The fundamental question for modeling LOC with CFD is what level of accuracy is needed from CFD data to meet the FAA stall training requirements, i.e., how good is good enough? There have been a number of attempts to establish these guidelines. One systematic study of pilot responses to several stall models for commercial transport training is reported in Ref. [13]. This study utilized a sampling of 9 test pilots and 45 airline pilots with stall experience to evaluate 3 stall models in a high-fidelity B-737 flight simulator. It was concluded that B-737 stall characteristics from a "representative" model created from computational aerodynamic and wind-tunnel data were generally similar to that of a "specific" model created from B-737 flight stall data. Also, the applicability of using a "representative" model in instances when a "specific" model is not available appears practical, considering their similarities. A more detailed description of the "representative" modeling approach is described in References [12] and [13].

From these characterizations of stall models, one important contribution from CFD-derived data would be to correctly capture the dynamic responses in roll, pitch, and yaw of a specific aircraft approaching, entering, and recovering from stall at the relevant flight conditions. The end goal is to create an acceptable representation of the behavior and response of the aircraft around the stall boundaries to a level of fidelity of the "representative" model as described in Ref. [13]. Hence, the present investigations have focused on time-accurate Reynolds Averaged Navier-Stokes (RANS) solutions to separated flows that are more cost effective than the more advanced eddy simulation models, which are at least an order of magnitude more computationally expensive. It is well known that RANS produces a smoothed, averaged representation of separated flow. But for the purposes of augmenting flight

simulator models using CFD results that capture the general behavior of stall, the RANS formulation is being investigated as a plausible level of fidelity for a "representative" model.

IV. NASA Generic Transport Model (GTM)

The focus configuration for the Aviation Safety Program is a representative twin-engine commercial transport configuration called the Generic Transport Model (GTM), shown in Figure 1. This configuration has undergone multiple wind-tunnel tests at NASA LaRC to characterize its aerodynamics at large angles of attack and sideslip, investigate the effects of airframe damage, and to examine its dynamic responses to forced oscillating motions in the wind tunnel that allow modeling of the conditions experienced during loss-of-control accidents. Over 50,000 data points have been obtained using static and dynamic testing methods. The GTM has also been flown as a 5.5% sub-scale flight model, called AirSTAR, to better replicate the actual flight dynamics of the aircraft [14] to [17].

The primary GTM force and moment tests were conducted in the 14X22 Foot Subsonic Wind Tunnel (14X22) on a 5.5% scale model at sea level atmospheric conditions with a dynamic pressure of 10 psf, corresponding to a freestream Mach number =0.08, chord Reynolds number Re_{cref} =0.54x10^6, and up to 85° angle-of-attack and +/-45° sideslip [2] to [7]. Boundary-layer transition grit was applied on the upper and lower surfaces of the wing, horizontal and vertical tails, and fuselage nose. But there was no verification that the flow had been tripped. The 12 Foot Low Speed Tunnel (12FT LWT) data [8] for the GTM was measured on a 3.5% scale model at dynamic pressure of 4 lb/ft^2 with approximate Mach number =0.05 and chord Reynolds number 0.25x10^6 with no transition grit applied.

V. Computational Tools

Two unstructured Navier-Stokes flow solvers based on fundamentally differing high-fidelity methodologies are exercised in this study. Both codes are being applied to fully tetrahedral unstructured grids. One code (TetrUSS/USM3D) [35], [36] solves the flow equations at the tetrahedral cell centers, whereas the other (FUN3D) [37], [38] solves them at the cell vertices or nodes. Both codes have an array of established 2nd-order time stepping schemes, upwind flux methodologies, and turbulence models. The Spalart Allmaras (SA) and Menter Shear Stress Transport (SST) turbulence models were used for the present work. The utilization of two codes allows for an assessment of numerical uncertainty of results from fundamentally different discretization and grid strategies. They do not, however, address the uncertainty of modeling errors of RANS.

The USM3D flow solver has been installed as a plug-in to the FD-CADRE framework (Fluid Dynamics – Computational Analysis of Dynamically Responsive Environments) [39] developed at Arnold Engineering Development Center in Tullahoma, Tennessee to control grid motion for dynamic cases. FD-CADRE is a generalized dynamic process control manager for coupling various plugins, e.g., flow solver, 6-DOF-motion generator, aeroelastic structural module, etc.

The computational grids were generated with the VGRID tetrahedral grid generator [40], [41] that is based on the Advancing Front Method (AFM) for generation of surface triangles and 'inviscid' field cells, and the Advancing Layers Method (ALM) for generation of thin-layered 'viscous' cells. Both methods are based on marching processes in which tetrahedral cells grow from an initial front (triangular surface mesh) until the volume around the geometry is filled. Unlike the conventional AFM, which introduces cells into the field in a totally unstructured manner, the ALM generates organized layers of thin tetrahedral cells, one layer at a time, while maintaining the flexibility of AFM. A typical surface mesh on the GTM is shown in **Figure 2**.

VI. Aerodynamic Analysis for LOC

A. Off-nominal conditions

Early calibration studies were conducted to assess the utility of the USM3D and FUN3D flow solvers for predicting aerodynamics of the GTM at off-nominal conditions and with dynamic motions. Tetrahedral grids were constructed for the GTM configuration, appropriate to each flow solver, with an attempt to achieve comparable spatial discretization between codes, i.e., similar number of tetrahedral cells for USM3D as cell vertices for FUN3D. Half-span grids ranged from 6-, 12-, and 24-million degrees of freedom, with full-span grids generated by mirroring the half-span grids (Figure 2).

The very low Mach and Reynolds numbers of the experimental data, Refs [2] to [8] presented the greatest challenge with the correlations. While boundary-layer transition grit was applied to the 5.5% GTM model for the 14X22 tests, there was no verification that the flow had been tripped. Furthermore, oil flow images for the 3.5% scale GTM model in the 12FT LWT revealed substantial laminar separation bubbles along the leading edge [8]. The

computational solutions were run using the SA and SST turbulence models assuming fully turbulent flow at M_∞=0.2 and at the 14X22 Reynolds number Re_{cref} =0.54x10^6. All solutions, both static and dynamic, were computed with free-air far field boundary conditions and advanced with the time-accurate RANS formulation. While not the optimal experimental data set for CFD correlation, it is the most comprehensive set of its kind that is available.

1. Stall / high angle-of-attack

The initial GTM studies began with running the USM3D flow solver over an angle-of-attack range up to 40° with the SA and SST turbulence models. Solutions were generated at angles of attack of 4, 10, 14, 20, 24, 35, and 40 degrees on half-span grids of 6-, 12-, and 24-million cells. Results presented in Ref. [42] demonstrate that the sensitivity of the solution to grid density was essentially negligible compared to that from the two turbulence models. The impact of turbulence model on static lift and pitching moment coefficients is addressed in **Figure 3** for the 6-million cell half-span grid. The dominant effect is in the stall region beyond α=10°. Predicted lift for the SST model is significantly below that of the SA model and experimental data over angle-of-attack range from 14° to 24°. Significant differences persist at the higher angles of attack with the SST model correlating best at α=40°. The SST model is known to produce lower levels of turbulent viscosity than the SA model for massively separated flows, thereby allowing disturbances to propagate more readily to the wing upper surface.

The behavior of the GTM wing surface flow patterns through stall is shown in **Figure 4** relative to the C_m and C_L coefficients. Solutions were generated at Δα=1° increments between angle-of-attack 4° and 14° with finer resolution in the region of stall between angle-of-attack 11° and 12°. As evident in the surface flow traces, wing separation starts at the trailing edge and progresses forward with increasing angle-of-attack. An abrupt, full upper surface separation occurs with angle-of-attack increasing from α=11.75° to 12°. The stall is less abrupt for the 14X22 experimental coefficients, most likely because of the very low Mach and Reynolds number flow. A surface oil flow on the 3.5% scale GTM at α=12° from the 12-Foot Low-Speed Wind Tunnel (12FT LWT) test [8] is included in the lower right of Figure 4. The experimental flow remains attached further outboard of the nacelle than in the computational solution, but is fully separated over the outer portion of the wing in both cases. Once again, these differences are likely caused by not tripping the boundary layer at the very low chord Reynolds number (0.25 million) in this test. Substantial laminar separation bubbles were observed along the GTM leading edge in other oil flow images from this data set [8]. While fraught with challenges, these correlations were pursued to generate some level of understanding for applying the RANS methodology to stalled, fully-separated flows using the only data of its kind available. This inconsistency should be mitigated when computing configurations at full-scale flight conditions.

The effect of sideslip in the vicinity of stall was also examined for the GTM in the full-span mirrored grids. Surface flow traces are shown in **Figure 5** depicting the effect of sideslip β from 0° to 10° nose left at the critical stall angle-of-attack, α=12°. Similar sequences were also generated for α=10°, 11°, and 13°, but are not shown. At β=0°, the wing is in full stall. At β=2°, a significant asymmetry develops just outboard of the nacelles. At β=4° and beyond, the left wing panel becomes more attached, whereas the same region on the right wing maintains a surface vortex separation. In **Figure 6,** the α=12°, β=4° flow traces are compared to the oil flow patterns from the 12-FT LWT data. Many similarities can be observed in asymmetric patterns between the CFD and experiment.

2. Airframe damage

Reference [43] presents a correlation study of two unstructured Navier-Stokes flow solvers, USM3D and FUN3D, with experimental wind-tunnel data [7] for the GTM with simulated damage to the wing, vertical tail, and horizontal tail. The objectives were to 1) evaluate the accuracy and utility of the respective numerical tools by correlating with wind-tunnel data for a "damaged" subsonic transport configuration, and then 2) establish application guidelines for simulating aircraft experiencing wing, vertical tail, and horizontal tail damage. Sample results for damage to the vertical- and horizontal-tail are highlighted in the following.

The effect of progressive vertical tail (VT) tip losses of 12.5%, 25%, 50%, and "No VT" on the lateral stability derivative, C_{n_β}, is presented in **Figure 7**. Reference [43] includes an excellent correlation of USM3D and FUN3D results with experimental data that capture the effect of vertical tail loss on yawing moment coefficient (C_n) vs. angle-of-sideslip (β) at α=0°. The static directional stability derivative term, C_{n_β}, for both experiment and CFD, shown in Figure 7, was computed as the linear slope of C_n between sideslip angles of -4^o and +4^o. The effect of vertical tail tip loss is a progressive degradation of directional stability as evidenced by the decrease in C_{n_β} and, as expected, a complete loss of directional stability (negative C_{n_β}) for the "No VT" case. A very good correlation with the experimental data is observed for both flow solvers.

The impact of progressive left horizontal tail (HT) tip losses of 12.5%, 25%, 50%, and 100% on longitudinal static margin about the 25-percent mean aerodynamic chord, *mac,* is characterized in 8. Static margin, derived from the slope of C_m vs. C_L, is commonly used to characterize the static stability and controllability of aircraft, and is defined as the distance between the center of gravity and the neutral point of the aircraft. **Figure 8** depicts the decreasing static margin due to increasing horizontal tail loss. Beyond approximately 70% tip loss, the aircraft exceeds its aft center of gravity limit and cannot be controlled. The computational data from USM3D (open symbols) and FUN3D (solid symbols) are in reasonably good agreement with the 14X22 experimental data (line symbol).

A Rapid Assessment of Airframe Damage, or RAAD, method [44] has been developed that quickly and accurately estimates a broad range of airframe damage conditions in a matter of seconds, rather than in hours as required by CFD solutions. The method makes use of the CFD solutions for the undamaged configuration across a range of flight conditions, and re-integrates the forces and moments in a manner that approximates the effects of a prescribed damage. Typical results produced by the RAAD method are captured in the dashed line on Figure 8. These estimates of horizontal tail tip loss of the GTM were produced in seconds and generally agree well with CFD prediction of the damaged configuration for moderate damage, but discrepancies can grow as the extent of the damage increases. This method provides a powerful engineering tool for estimating airframe damage from baseline CFD solutions. An analysis of the GTM for 12 damage scenarios at 17 flight conditions required about 30 seconds on a typical workstation.

3. Atmospheric / Environmental

Atmospheric gusts and wind shear, and the accumulation of ice along wing leading edges represent significant threats for aircraft loss-of-control. Statistics compiled in Ref. [1] for aircraft LOC accidents occurring between 1979 and 2009 identify 18 mishaps caused by wind shear, gusts, and thunderstorms producing 1126 fatalities, and 28 accidents related to icing responsible for 595 fatalities.

Icing

Since the early 1990s, NASA Glenn Research Center has sustained a strong research effort to develop validated experimental and computational simulation methods suitable for evaluating aircraft operating in icing conditions. Considerable resources have been directed toward creating a validated icing tool called LEWICE3D [45] that models droplet trajectory and heat transfer to predict the rate and shape of ice accumulation along leading edges of aerodynamic surfaces. LEWICE3D is continually being refined through calibration with experimental aircraft icing data and improved gridding techniques [46] to [48]. In support of the AvSafe program, this tool was used to create icing shapes for the GTM configuration for testing in the NASA LaRC 12-FT LWT [8]. Although tested at very low Mach and Reynolds number, these data represent an initial attempt to obtain aerodynamic data on the GTM with computationally designed artificial ice shapes over a large range of angle of attack and sideslip. The testing included the measurement of aerodynamic force and moments, and qualitative surface oil flow information.

Researchers at NASA Glenn are currently coordinating collaborations between NASA, FAA, Boeing, the University of Illinois, and the French Aeronautics and Space Research Center, ONERA [49] to address the technical challenges associate with icing on large-scale three-dimensional swept wings. The overall goal is to improve the fidelity of experimental and computational simulation methods for modeling the aerodynamic effects of swept-wing ice accretion formation. One of the objectives under this collaboration is to generate a database of 3-D, swept-wing, ice-accretion geometries for icing-code development and validation and for aerodynamic testing on an open-domain geometry representative of current, modern civilian transport airplanes. The Common Research Model (CRM) [50] was selected for this effort since it has been widely used and accepted by the international community through the NASA/AIAA Drag Prediction Workshops [51].

Gusts

Computational methodologies are available for modeling the effects of wind gusts on airframe aerodynamics [52]. Gust models have been implemented into two prominent CFD flow solvers, the NASA FUN3D code [53], [54] and the European Tau code [55]. After a review of the literature, most applications of gust modeling are related to the prediction of airframe load responses [54], [55], rather than to the destabilizing impact of gusts at LOC flight conditions. Hence, gust response on flight dynamics in the vicinity of stall is a phenomenon affecting the safe flight of civil transports that may warrant further consideration.

B. Lessons for Dynamic Simulations

A systematic study is presented in Reference [42] using the NASA GTM to guide the selection of a numerical solution strategy for time-accurate RANS computation of a subsonic transport configuration undergoing simulated forced oscillation about its pitch axis, as shown in **Figure 9**. This study benefitted from a direct transfer of lessons learned during a parallel guideline study on the NATO STO AVT-161 SACCON UCAV configuration [56]. Forced

oscillation is central to the prevalent wind-tunnel methodology for quantifying aircraft dynamic stability derivatives from force and moment coefficient measurements, which is the ultimate goal for the computational simulations. Figure 9 conveys the response of the pitching moment, C_m, and the regions of flow separation, denoted by green isosurface representing zero streamwise velocity, above the lifting surfaces due to a $\Delta\alpha$=+/-5° sinusoidal oscillation of frequency 0.43Hz for the GTM about the nominal post-stall angle-of-attack, α_0=24°. The directions of upswing and downswing are denoted. The flow over the oscillating wing forms a time-lagged response, evident in the corresponding flow images, which causes the C_m at α_0=24° to be larger on the downswing and lower on the upswing. The ΔC_m at 0° body angle (α_0=24°) represents the dynamic response to motion and is used in constructing the dynamic derivative.

Some critical lessons were learned during this study for applying USM3D for dynamic applications. The studies of references for the GTM [42] and for the SACCON [56] each applied a systematic approach to assess the accuracy of using 360, 720, and 1440 time steps per pitch cycle with the varying numbers of inner iterations between the 2nd order time step. The example shown in **Figure 10** from the GTM study depicts the C_m vs. $\Delta\alpha$ responses to sinusoidal pitch motion $\Delta\alpha$=+/-5° about α_0=24° for three oscillation frequencies 0.43Hz, 0.12Hz, and 0.05Hz. These results demonstrate the ability of CFD to generally capture the effects[1] of oscillation frequency with the SA turbulence model. Furthermore, these results convey the solution sensitivity from varying inner iterations between 100, 50, and 30 for the time discretization of 360 steps per cycle. The approach was to first establish an ultra-converged solution, which in this case was the combination 360/100, and then decrease the numbers of inner iterations in order to determine the suitable range for good convergence. It was conclusively demonstrated during the studies in [42] and [56], that the convergence of periodic oscillating solutions with USM3D is a function of the total numbers of solutions iterations, i.e., (number of time steps per cycle)*(number of inner iterations), independent of configuration. Identical results are generated with the combinations 360/100, 720/50, and 1440/25. There are apparently no shortcuts to convergence. An efficient systematic strategy for guiding the selection of a numerical strategy for applying RANS computations of configurations undergoing simulated forced oscillations is reported in [42] and [56].

VII. Progress Toward Full-Maneuver CFD Flight

Exponentially increasing high-performance computing capabilities over the past several decades have perpetuated the vision of direct flight simulation [57] where an aircraft is "flown in the computer" by carrying out unsteady maneuvers using the equations of motion in physical time subject to responses from control surface deflection, engine power, and aeroelastic deformation. Significant advances in this capability have been demonstrated on coarse grids under the US Air Force Computational Research and Engineering Acquisition Tools and Environments (CREATE) Program [58] using the Kestrel flow solver [59], and the German DLR Digital-X Project using the Tau flow solver [60]. Forsythe et al. [61] demonstrated an impressive simulation of a UH60 helicopter approaching through the airwake and landing on the back of a ship. This was accomplished through a creative coupling of the Kestrel flow solver with the U.S. Navy flight simulation executive, CASTLE. Such simulations could conceivably lead to increased safety by capturing the true flight dynamics of an aircraft undergoing loss-of-control. Unfortunately, the limits imposed by extreme computer resource requirements will most likely impede the full application of direct flight simulation for the foreseeable future. A balanced interim solution is to dedicate sufficient resources toward advancing the hybrid approach of creating high-fidelity ROMs from CFD solutions.

VIII. Progress Toward Reduced-Order Modeling

The goal of a reduced-order model is to provide an accurate representation of the full unsteady and nonlinear flight dynamic characteristics of an aircraft within seconds. Several approaches being explored under the AvSafe and Airspace Operations and Safety Programs are summarized in the following.

A. NCSU Research in Low-Order Stall Prediction

Researchers at the North Carolina State University (NCSU) are investigating approaches for rapidly modeling the effects of static and dynamic post-stall aerodynamic behavior using lower-order potential flow tools, such as the vortex lattice method (VLM) or lifting line theory, augmented to handle corrections for viscous effects. At the core of this effort is a novel iterative decambering approach [62], [63] for prediction of post-stall characteristics of wings

[1] The vertical offset of hysteresis loops is related to differences in static C_m correlations. The size and shape of the loops are the important indicators of dynamic behavior.

using known viscous section data (C_l and C_m vs. α) as inputs. In this approach, a camber reduction, or "decambering," is applied to each section of a wing to mimic the effective camber change due to boundary-layer separation at and beyond stall. This decambering is modeled using a function of one or two variables. On an airfoil section, the decambering is determined such that the potential flow past the decambered airfoil at some α will result in the same C_l and C_m values as those resulting from the viscous flow past the actual airfoil (determined either computationally or experimentally for that α). On a wing or multiple-lifting-surface configuration, using a strip-theory approach, the decambering on each section is determined such that the zero-normal-flow boundary conditions are satisfied at the control points of all sections of the wing while also ensuring that the predicted C_l and C_m for each section match with the viscous section data provided as input. These conditions are satisfied using an iterative approach, which is discussed in more detail in [63]. This procedure is rapid, and it converges in a fraction of a second for a given post-stall operating condition with specified values for α, β, and angular velocities. As a result, "in-the-loop" aerodynamic calculations are possible for real-time simulation of flight dynamics even at post-stall conditions. **Figure 11** from [64] shows early predictions for the trajectories for an example airplane configuration with rectangular and tapered planform options for the wing geometry. In each case, one minute of the post-stall flight dynamics, simulated following rudder and up-elevator input applied at a near-stall trim condition, took less than 20 seconds of run time on a modest laptop computer even though the post-stall aerodynamics calculations were performed at every time step of the simulation.

In another recent effort [65], the decambering approach was incorporated in an unsteady vortex lattice method for flight-dynamics analysis of rigid aircraft. In this analysis, linearization of the aircraft dynamics equations is carried out for a pre- or post-stall trim condition, leading to a state-space system in which the state vector comprises the incremental vortex-lattice circulations, the rigid body velocities, and the Euler angles. Decambering is introduced into the system matrices in post-stall flight conditions by treating it at each strip as a control effector, whose deflection is linearly related to the flight velocities (translational and rotational). The relationship between the change in flight velocities and the change in decambering is appended to the system in feedback form. Eigenvalue analysis of the resulting system matrices yields the flight dynamic modes of the vehicle. Results for loss of roll damping with increase in angle of attack beyond stall showed excellent agreement with high-α data from flight-test results in the literature. Full-aircraft results for all flight modes were verified for pre-stall conditions. At post-stall conditions, the full-aircraft predictions for some modes were in broad agreement with the limited general trends that could be found in the literature.

While the decambering approach is promising, it is necessary to validate the decambering approach and find the limits beyond which the current approach will not work. Further validation is also needed for the predicted flight dynamics. Because the decambering approach uses viscous section data as inputs and predicts wing/configuration forces and moments as outputs, validation requires consistent datasets for both inputs and outputs. The dearth of consistent airfoil and wing experimental data extending into post-stall regimes provided the impetus to develop a systematic dataset using RANS CFD [66]. When airfoil section data from the CFD was used as input, it was seen that the forces, moments, and spanwise loadings for unswept wings predicted by the decambering method matched quite well with those from CFD [63]. However, predictions for swept wings from the decambering approach showed progressive deviation from the corresponding CFD results as sweep angle was increased [63]. As is well known [67], [68], [69], spanwise pressure gradients on aft-swept wings cause tipward propagation of separated flow at and beyond stall. As a result, inboard sections of highly swept wings have attached flow even well after the wing has stalled, and have local C_l exceeding section $C_{l,max}$. The tip regions, on the other hand, experience premature stall and low section $C_{l,max}$. **Figure 12** shows CFD results for upper-surface skin-friction lines for an unswept and a 30-degree swept wing at a post-stall angle of attack of 18 degrees. While the skin-friction lines for the unswept wing are in the chordwise direction, the tipward propagation of the separated surface flow on the swept wing is evident. The effect of separated-flow propagation on the section lift behavior of swept wings invalidates the main assumption in the current decambering method that the relationship between local C_l and effective α on all sections of a finite wing is practically the same as the relationship between C_l and α for the corresponding airfoil. Extensions to the decambering approach to handle swept wings are being pursued in on-going research. As shown in [70], when the input section lift curves are corrected using information deduced from swept-wing CFD results, the results from the decambering approach agree remarkably well with those from the swept-wing CFD analyses. The challenge is to develop a completely predictive decambering approach for swept wings in which the need for wing CFD results to develop the corrections are kept to a minimum or avoided entirely. On-going research, funded by the NASA TASEAS project, is focused on such a goal.

B. LaRC Research in Unsteady Modeling Using Wind-tunnel and Computational Data

Researchers commonly use System Identification (SID) methods to obtain stability and control derivatives useful for flight dynamics analysis and design applications, such as simulation and flight control design. SID is a body of theory used to identify mathematical model structures and model parameters in a statistically rigorous manner that describes the relationship between input and output data of dynamic systems of interest. The mathematical structures can take various forms depending on the intended use. Aircraft SID is well documented in Ref. [71]. With the advent of modern CFD capabilities, research is underway to identify approaches for using computational data in combination with SID. At LaRC, research to further develop SID methods in application to computational, flight, and ground-based approaches to modeling is ongoing. Initial efforts to capitalize on CFD capabilities using SID research, [72] to [74], are highlighted in this section. In these studies, indicial-modeling techniques, found effective in dynamic wind tunnel testing, were utilized in application to CFD to allow higher fidelity ROM estimation. A more detailed review of the nonlinear unsteady modeling work at LaRC using ground-based testing and CFD simulated data is given in Ref. [75].

Predicting aircraft response in nonlinear unsteady flight regimes is an ongoing area of research. This region of the flight envelope is typically observed during maneuvers at high angles of attack with separated flows. Validation of analytical models for dynamic response is typically accomplished by comparing time histories of predicted and measured responses. However, this approach may not guarantee a match with the underlying physics. An early effort [72] was made to resolve this issue by comparing parameters from the underlying models (ROMs) that captured the dynamics observed in both the predicted and measured models. By introducing SID methods, this approach also allowed uncertainty bounds to be introduced to both the computational and wind-tunnel model parameters. Uncertainty information is not commonly provided in conventional wind-tunnel or computational results, however, uncertainty bounds provide important information about the quality and character of the mean values presented. Although computational results are deterministic, the results still include a number of sources for systematic and modeling errors. Since application of least-squares methods does not require an assumption of a particular noise distribution in the measurements, the estimated uncertainty bounds can still reflect modeling and systematic errors.

An example of SID applied to both CFD simulated data and wind-tunnel data is shown in **Figure 13** [72]. In this case, an unsteady model for the roll moment coefficient was estimated for the SACCON model undergoing forced-oscillations in the LaRC 14x22 wind tunnel. Classical S&C derivatives for roll damping and effective dihedral are shown on the left side of the figure. On the right side, two parameters define an unsteady transfer function that captures a lag in the roll response. The single-pole transfer function is defined by a, a gain on the transfer function, and τ_1, a time constant. The three small circles and vertical bars correspond to the mean values and 2σ error bounds, respectively. WT refers to the wind tunnel based model. SA and SST refer to the two turbulence models chosen for this study. A notable result for this study was that the uncertainty bounds overlapped for the conventional derivatives. This implies no statistical difference exists between the three parameters at the 95% confidence level. The transfer function time constant was in statistical agreement using the wind-tunnel and SA models. For the attenuation factor, statistical agreement was found for the SA and SAA models but not with the WT model.

An additional study [74] investigated roll instability in the NASA GTM model where a significantly greater understanding of the aerodynamics was brought to light by use of SID and CFD. The roll instability was observed at $\alpha = 12°$ in the wind tunnel. The instability was also observed in flight [76] and characterized as a roll-off departure at 14° angle of attack. As part of the study [74] harmonic analysis was used to characterize and understand the roll damping in both the wind-tunnel and CFD simulation. Figure 4 presents a sharp break in the lift curve at $\alpha = 12°$ and **Figure 14** presents harmonic analysis results where the out-of-phase term (damping) for the roll moment shows a clear instability in the region $12° \leq \alpha \leq 15°$. This work extended aerodynamic characterization of the GTM model and confirmed results from flight and wind tunnel.

C. DoD Research in Reduced-Order Modeling (ROM)

The biggest challenge for creating a ROM from CFD is the need to generate a large number of flow solutions to resolve any combination of angle-of-attack, sideslip and free-stream Mach number within the flight envelope. If ever to be practical, efficient techniques must be developed to limit the amount of computational work required to create nonlinear ROMs. Two promising efforts underway within the Department of Defense (DoD) community are reviewed in the following. Since the DoD focus is on high-performance military aircraft that routinely encounter highly nonlinear flight conditions, these technologies are especially beneficial to NASA's goals of modeling the nonlinear flight dynamics of civil aircraft undergoing loss-of-control.

1. U.S. Air Force Seek Eagle Office (AFSEO)

For several years, the AFSEO has been exploring innovative S&C analysis processes to efficiently utilize dynamic CFD solution data in the SID model development process for complete aircraft configurations. One such

approach [77] illustrated in **Figure 15** begins with a CFD representation of the complete aircraft of interest (including stores, control surfaces, etc.). This configuration is flown through training maneuvers designed to excite the relevant flow physics that will be encountered during actual missions in all three axes (roll, pitch, and yaw). These simulations are termed "training maneuvers," since the actual combinations of translations and rotations during the maneuvers are often not physically possible to achieve by an actual aircraft in flight or during a wind-tunnel test. Next, SID techniques are applied to create a mathematical model of the aircraft response. Then, the model is tested against realistic CFD simulations and available experimental data to verify its validity. If not satisfactory, then the process is repeated with other training maneuvers. This method may also be used in conjunction with flight test. Predictions of desired flight-test points are made using the model before flight tests are conducted to determine the expected behavior of the actual aircraft and possibly to even omit certain flight-test conditions. While innovative, this approach does tend to require a large amount of computational resources to fly the various maneuvers during the trial-and-error process. Furthermore, the published models are based on multi-dimensional polynomials that do not have a direct connection to the classical models based on stability derivatives.

2. United States Air Force Academy (USAFA)

Through their participation in the NATO STO AVT-201 task group, Ghoreyshi and others at the United States Air Force Academy are exploring the creation of nonlinear ROMs from CFD using the indicial response functions, [18], [32], [78] to [83]. The time-dependent longitudinal aerodynamic force and moment coefficients are expressed in Eq. 1 as a function of angle-of-attack and Mach number, where *j=L,m* denotes lift and pitching moment

$$C_j = C_{j0} + \frac{d}{dt}\left[\int_0^t C_{j\alpha}(t-\tau\,,\alpha,M)\alpha(\tau)d\tau\right] + \frac{d}{dt}\left[\int_0^t C_{jq}(t-\tau,\alpha,M)q(\tau)d\tau\right] \quad (1)$$

The lateral/directional coefficients are expressed in Eq. 2 as a function of angle-of-attack, sideslip, and Mach number, where *k=Y, l, n* denote the side force, rolling moment, and yawing moment

$$C_k = \frac{d}{dt}\left[\int_0^t C_{k\beta}(t-\tau\,,\alpha,M)\beta(\tau)d\tau\right] + \frac{d}{dt}\left[\int_0^t C_{kp}(t-\tau,\alpha,M)p(\tau)d\tau\right] + \frac{d}{dt}\left[\int_0^t C_{kr}(t-\tau,\alpha,M)r(\tau)d\tau\right] \quad (2)$$

The angular derivatives, $C_{j\alpha}(t)$ and $C_{k\beta}(t)$ are modeled by indicial responses to a unit step change in angle-of-attack and sideslip, respectively. The rate derivatives, $C_{jq}(t), C_{kp}(t)$, and $C_{kr}(t)$ are modeled by indicial responses to a unit step change in pitch, roll, and yaw rate, respectively. One advantage of this approach with CFD is the ability to use grid motion to uncouple the angular and rate terms. For example in **Figure 16** using two established RANS flow solvers, *Cobalt* [84] and USM3D [35], a unit step change in angle-of-attack is produced when the grid impulsively starts to move downward and aft in a way that removes any effect from rotation rate. Similarly, for a unit step change in pitch rate, the grid translates and rotates simultaneously along a curved trajectory that maintains α=0° while rotating in pitch at a constant rate. For each of these trajectories, the motions continue until the flow adjusts to a new steady state.

Generating the derivatives in Eqs. 1 and 2 over a range of α and *M*, e.g., $C_{j\alpha}(t,\alpha,M)$, will capture many of the nonlinearities within the flight envelope. Ghoreyshi et al. [78] incorporated a method to efficiently reduce the required number of step function calculations using a time-dependent surrogate model to fit the relationship between flight conditions (Mach number, angle-of-attack, and sideslip) and step functions calculated from a limited number of simulations (samples). A set of indicial response solutions is generated at pre-determined values of α and *M* as illustrated in **Figure 17**. This matrix of cases can be determined using Design of Experiment techniques, or from prior knowledge of the nonlinear regions of the flight envelope. The set of responses is interpolated using a technique such as Kriging to determine the time-dependent indicial responses across Mach number, angle-of-attack, and sideslip. Hence the required number of indicial solutions depends on the level of granularity required to resolve the nonlinearities of the flight envelope. In practice, a surprisingly small number of solutions are required to generate a reasonable nonlinear model [83]. In most cases, it is less expensive to generate the CFD solutions for creating the ROM than to "fly the CFD" through a full flight maneuver. Furthermore, once the ROM has been generated, it can be flown through multiple maneuvers within seconds. The ROM used to fly the AVT-201 SACCON UCAV configuration through Lazy-8 and Immelmann maneuvers shown in **Figure 18** was created from *Cobalt* indicial solutions at 33 sample points [78], [83]. Once the ROM was constructed, it was used to generate results for the Lazy-8 and Immelmann maneuvers within seconds that were in excellent agreement with full CFD *Cobalt* flight solutions that each required approximately 50,000 CPU hours. Similar successes were also achieved on the X-31 aircraft [80], [83]. One additional advantage of this approach is its ability to model the unsteady responses from control surface deflections [82].

Collaborations are underway between NASA and USAFA through the NATO STO AVT-201 task group to infuse this new CFD-to-ROM methodology into the Aviation Safety Program for LOC modeling of civil aircraft. The USAFA has generously provided their coding for generating the indicial maneuvers, which in turn have been adapted to the NASA USM3D/FD-CADRE system. An initial correlation study of USM3D with flow solvers from USAFA and The National Aerospace Laboratory (NLR) in The Netherlands using the NACA 0012 airfoil and the AVT-201 SACCON configurations is presented in Ref. [32].

IX. Recommendations

The following recommendations are offered for advancing the application of CFD toward creating ROMs for civil aircraft LOC simulations.

1. More resources should be directed toward maturing methodologies for creating high-fidelity nonlinear ROM's from CFD. Progress is being made in the full-maneuver CFD flight, but the limits imposed by extreme computer resource requirements will most likely impede its practical application to LOC flight simulation training for the foreseeable future.
2. The NATO/USAFA approach of using indicial maneuvers that separate the angular and rate derivatives in conjunction with the surrogate model approach is particularly promising. Collaborations with the USAFA should be continued to exploit this new technology for creating LOC flight simulation training models.
3. There are no investigations recorded in the literature on the impact of wind gusts affecting aircraft operating in the region of stall and LOC. This topic should be considered in future work.

X. Concluding Remarks

A concerted effort has been underway over the past several years within the NASA Aviation Safety Program to evolve computational capabilities for modeling aircraft loss-of-control. The motivation stems from a new FAA requirement that enhanced flight simulator models be implemented by early 2019 for training pilots to recognize precursors to stall and to learn strategies for upset recovery. The primary challenge arises from the conflicting requirements that flight simulators operate in real time in response to pilot input whereas advanced computational tools generally require hours to generate data for one point. Hence, the approach is limited to 1) finding efficient ways to utilize high-fidelity CFD data in the generation of reduced-order models that augment flight simulator models at LOC conditions, and 2) developing very fast low-order LOC approximation tools that can run in real time.

A principle goal guiding the present work has been to develop reliable computational tools for predicting and analyzing the non-linear stability & control characteristics of aircraft near stall boundaries affecting safe flight, and for utilizing those predictions for creating augmented flight simulation models that improve pilot training. Addressing such an ambitious goal with limited resources required a strategy to leverage the expertise and resources of other researchers and organizations. Hence, close collaborative relationships were forged with a diverse body of computational aerodynamicists and flight simulation experts to leverage their respective research efforts into the creation of NASA tools to meet this goal. As a result, considerable progress has been made with limited resources, although much work remains to be done.

A range of studies were initially conducted to correlate CFD and wind-tunnel data of the NASA Generic Transport Model at extreme angles of attack and sideslip, with airframe damage, and under dynamic motion. From this, a new method for rapidly analyzing the aerodynamic degradation due to airframe damage was developed. The applicability of CFD for predicting aircraft dynamic stability and control was thoroughly investigated through the collaborative efforts of over 40 researchers from 14 countries and 7 CFD codes under the NATO STO AVT-161 and AVT-201 task groups. This research was infused directly into the AvSafe Program and ATD project aircraft LOC work in an on-going basis.

Parallel studies were carried out in search of ways to apply CFD-derived data to system identification techniques for constructing reduced-order models. These studies were conducted partly internally within NASA, and also collaboratively with the NATO technical working groups. A particularly promising approach to creating LOC ROM's from CFD was devised under AVT-201 that warrants further investigation. While the majority of effort was focused on high-fidelity CFD, the TASEAS work is also supporting researchers at North Carolina State University to mature a promising approach for real-time prediction of aircraft stall using low-order computational tools.

Acknowledgments

The work reported herein is currently funded by the Technologies for Assuring Safe Aircraft Energy and Attitude State (TASEAS) work element under the NASA Airspace Operations and Safety Program, Airspace Technology Demonstration (ATD) project. The low-order post-stall modeling work at NCSU is supported under TASEAS work . The consistent support since 2007 from the Aviation Safety Program is greatly appreciated. The authors wish to express a special gratitude to Dr. Christine Belcastro of the Dynamic Systems and Control Branch and Mr. Gautam Shah of the Flight Dynamics Branch for their continued support and advocacy for this work across multiple program cycles.

References

[1] Belcastro, C.M. and Foster, J.V., "Aircraft Loss-of-Control Accident Analysis", AIAA 2010-8004.

[2] Shah, G.H., Cunningham, K., Foster, J.V., Fremaux, C.M., Stewart, E.C., Wilborn, J.E., Gato, W., and Pratt, D.W., "Wind-tunnel Investigation of Commercial Transport Aircraft Aerodynamics at Extreme Flight Conditions", SAE-2002-01-2912, November 2002.

[3] Cunningham, K., Foster, J.V., Shah, G.H., Stewart, E.C., Ventura, R.N., Rivers, R.A., Wilborn, J.E., and Gato, W., "Simulation Study of Flap Effects on a Commercial Transport Airplane in Upset Conditions", AIAA 2005-5908, August 2005.

[4] Foster, J.V., Cunningham, K., Fremaux, C.M., Shah, G.H., Stewart, E.C., Rivers, R.A., Wilborn, J.E., and Gato, W., "Dynamics Modeling and Simulation of Large Transport Airplanes in Upset Conditions", AIAA 2005-5933, August 2005.

[5] Murch, A.M. and Foster, J.V., "Recent NASA Research on Aerodynamic Modeling of Post-Stall and Spin Dynamics of Large Transport Airplanes", AIAA 2007-0463, January 2007.

[6] Shah, G.H., "Aerodynamic Effects and Modeling of Damage to Transport Aircraft", AIAA 2008-6203, August 2008.

[7] Shah, G.H., and Hill, M.A., "Flight Dynamics Modeling and Simulation of a Damaged Transport Aircraft", AIAA 2012-4632, August 2012.

[8] Broeren, A.P., Lee, S., Shah, G.H., and Murphy, P.C., "Aerodynamic Effects of Simulated Ice Accretion on a Generic Transport Model", SAE Technical Paper 2011-38-0065, June 2011.

[9] Q*ualification, Service, and Use of Crewmembers and Aircraft Dispatchers; Final Rule*, 14 CFR Part 121, Federal Aviation Administration, Federal Register, Vol 78, No. 218, Nov. 12, 2013, http://www.gpo.gov/fdsys/pkg/FR-2013-11-12/pdf/2013-26845.pdf

[10] Wilborn, J.E., and Foster, J.V., "Defining Commercial Transport Loss-of-Control: A Quantitative Approach", AIAA 2004-4811, August 2004.

[11] Carbaugh, D., "Approach to Stall Simulator Training", AIAA 2010-7795, August, 2010.

[12] Gingras, D.R., Ralston, J.N., and Wilkening, C.A., "Improvement of Stall-Regime Aerodynamics Modeling for Aircraft Training Simulations", AIAA 2010-7793, August 2010.

[13] Schroeder, J.A., Burki-Cohen, J., Shikany, D.A., Gingras, D.R., and Desrochers, P., "An Evaluation of Several Stall Models for Commercial Transport Training", AIAA 2014-1002, January 2014.

[14] Morelli, Eugene A., and Grauer, Jared A., "Efficient Flight Testing and Modeling Techniques Under Loss-of-Control Conditions," to be published JGCD, 2016.

[15] Grauer, Jared, A. and Morelli, Eugene A., "Real-Time Dynamic Modeling Under Loss-of-Control Conditions," to be published JGCD, 2016.

[16] Jordan, T.L. and Bailey, "NASA Langley's AirSTAR Testbed: A Subscale Flight Test Capability for Flight Dynamics and Control Systems," AIAA-2008-6660, August 2008.

[17] Morelli, E.A., "Flight Test Maneuvers for Efficient Aerodynamic Modeling", AIAA 2011-6672, August 2011.

[18] Ghoreyshi, M., Jirásek, A. and M. Cummings, R.M., " Computational Investigation into the Use of Response Functions for Aerodynamic Load Modeling", AIAA Journal, Vol. 50, No. 6, June 2012. doi: 10.2514/1.J051428

[19] Cummings, R.M. and Schütte, A., "Introduction to the AVT-161 Air Facet: An Integrated Computational/Experimental Approach to UCAV Stability and Control Estimation", NATO/RTO-TR-AVT-161, Chapter 1, September 2012.

[20] Schütte, A., Cummings, R.M., Stern, F., and Toxopeus, S., “Summary of AVT-161, Lessons Learned and the Way Ahead”, NATO/RTO-TR-AVT-161, Chapter 26, September 2012.

[21] Cummings, R.M., "Introduction: SACCON Uninhabited Combat Aerial Vehicle Experimental and Numerical Simulations", *Journal of Aircraft*, Vol. 49, No. 6 (2012), pp. 1541-1541. doi: 10.2514/1.C032134

[22] Cummings, R.M. and Schütte, A., "Integrated Computational/Experimental Approach to Unmanned Combat Air Vehicle Stability and Control Estimation", Journal of Aircraft, Vol. 49, No. 6 (2012), pp. 1542-1557. doi: 10.2514/1.C031430

[23] Vicroy, D.D., Loeser, T.D., and Schütte, A., "Static and Forced-Oscillation Tests of a Generic Unmanned Combat Air Vehicle", Journal of Aircraft, Vol. 49, No. 6 (2012), pp. 1558-1583. doi: 10.2514/1.C031501

[24] Roosenboom, E.W.M., Konrath, R., Schröder, A., Pallek, D., Otter, D., Morgand, S., Gilliot, A., Monnier, J.C., Le Roy, J.F., Geiler, C., and Pruvost, J., "Stereoscopic Particle Image Velocimetry Flowfield Investigation of an Unmanned Combat Air Vehicle", *Journal of Aircraft*, Vol. 49, No. 6 (2012), pp. 1584-1596. doi: 10.2514/1.C031587

[25] Rohlf, D., Schmidt, S., and Irving, J., "Stability and Control Analysis for an Unmanned Aircraft Configuration Using System-Identification Techniques", *Journal of Aircraft*, Vol. 49, No. 6 (2012), pp. 1597-1609. doi: 10.2514/1.C031392

[26] Tomac, M., Rizzi, A., Nangia, R.K., Mendenhall, M.R., and Perkins, S.C., "Engineering Methods Applied to an Unmanned Combat Air Vehicle Configuration", *Journal of Aircraft*, Vol. 49, No. 6 (2012), pp. 1610-1618. doi: 10.2514/1.C031384

[27] Frink, N.T., Tormalm, M., and Schmidt, S., "Three Unstructured Computational Fluid Dynamics Studies on Generic Unmanned Combat Aerial Vehicle", *Journal of Aircraft*, Vol. 49, No. 6 (2012), pp. 1619-1637. doi: 10.2514/1.C031383

[28] Schütte, A., Hummel, D. and Hitzel, S.M., "Flow Physics Analyses of a Generic Unmanned Combat Aerial Vehicle Configuration", *Journal of Aircraft*, Vol. 49, No. 6 (2012), pp. 1638-1651. doi: 10.2514/1.C031386

[29] Cunningham, Jr., A.M., “Technical Evaluation Report – Air Facet”, NATO/RTO-MP-AVT-189, August 2012.

[30] Gorski, J.J., “Technical Evaluation Report – Sea Facet”, NATO/RTO-MP-AVT-189, August 2012.

[31] Cummings, R.M., and Schütte, A., “The NATO STO Task Group AVT-201 on ‘Extended Assessment of Stability and Control Prediction Methods for NATO Air Vehicles,” AIAA 2014-2000, June 2014.

[32] Ghoreyshi, M., Frink N.T., van Rooij, M., Lofthouse, A.J., Cummings, R.M., and Nayani, S., “Collaborative Evaluation of CFD-to-ROM Dynamic Modeling”, to be presented at 2016 Aerospace Science Conference, San Diego, California, January 2016.

[33] Luckring, J.M., and Boelens, O.J., “A Reduced-Complexity Investigation of Blunt Leading-Edge Separation Motivated by UCAV Aerodynamics”, AIAA Paper 2015-0061, January 2015.

[34] Frink, N.T., “Numerical Analysis of Incipient Separation on 53° Swept Wing”, AIAA Paper 2015-0288, January 2015.

[35] Frink, N.T., “Tetrahedral Unstructured Navier-Stokes Method for Turbulent Flows”, AIAA Journal, Vol. 36, No. 11, 1998, pp. 1975-1982.

[36] Pandya, M. J., Frink, N. T., Abdol-Hamid, K. S., Samareh, J. A., Parlette, E. B., and Taft, J. R., “Enhancements to TetrUSS for NASA Constellation Program,” *Journal of Spacecraft and Rockets*, Vol. 49, No. 4, 2012, pp. 617-631.

[37] Anderson, W. K. and Bonhaus, D. L., “An Implicit Upwind Algorithm for Computing Turbulent Flows on Unstructured Grids" *Computers and Fluids*, Vol. 23, No. 1, 1994, pp. 1-22.

[38] Nielsen, E. J., Aerodynamic Design Sensitivities on an Unstructured Mesh Using the Navier-Stokes Equations and a Discrete Adjoint Formulation, Ph.D. thesis, Virginia Polytechnic Institute and State University, Blacksburg, VA, 1998.

[39] Power, G.D. and Calahan, J.A., “A Flexibßle System for Analysis of Bodies in Relative Motion”, AIAA Paper 2005-5120, June 2005.

[40] Pirzadeh, S.Z., “Three-Dimensional Unstructured Viscous Grids by the Advancing Layer Method”, *AIAA Journal*, Vol. 33, No. 1, 1996, pp. 43-49.

[41] Pirzadeh, S.Z., “Advanced Unstructured Grid Generation for Complex Aerodynamic Applications”, *AIAA Journal*, Vol. 48, No. 5, 2010, pp. 904-915.

[42] Thompson, J.R., Frink, N.T., and Murphy, P.C., “Guidelines for Computing Longitudinal Dynamic Stability Characteristics of a Subsonic Transport”, AIAA 2010-4819, July 2010.

[43] Frink, N.T., Pirzadeh, S.Z., Atkins, H.L., Viken, S.A., and Morrison, J.H., "CFD Assessment of Aerodynamic Degradation of a Subsonic Transport Due to Airframe Damage", AIAA 2010-500, January 2010.

[44] Atkins, H.L. and Frink, N.T., "Rapid Analysis of Aerodynamic Degradation due to Airframe Damage", submitted for publication as a NASA Technical Memorandum.

[45] Bidwell, C.S., and Potapczuk, M.G., "Users Manual for the NASA Lewis Three-Dimensional Ice Accretion Code (LEWICE3D)," NASA TM 105974, 1993.

[46] Bidwell, C.S., "Icing Analysis of a Swept NACA 0012 Wing Using LEWICE3D Version 4.38", AIAA 2014-2200, June 2014.

[47] Bidwell, C.S., "Icing Calculations for a 3D High-Lift Wing Configuration", AIAA 2005-1244, January 2005.

[48] Thompson, D., Tong, X., Arnoldus, Q., Colins, E., McLaurin, D., Luke, E., Bidwell, C., "Discrete Surface Evolution and Mesh Deformation for Aircraft Icing Applications", AIAA 2013-2544, June 2013.

[49] Broeren, A.P., Potapczuk, M.G., Riley, J.T., Villedieu, P., Moens, Frederic, and Bragg, M.B., "Swept-Wing Ice Accretion Characterization and Aerodynamics", AIAA 2013-2824, June 2013.

[50] Vassberg, J.C., DeHann, M.A., Rivers, S.M., and Wahls, R.A., "Development of a Common Research Model for Applied CFD Validation Studies", AIAA 2008-6919, August 2009.

[51] Levy, D.W., Laflin, K.R., Tinoco, E.N., Vassberg, J.C., Mani, M., Rider, B., Rumsey, C.L., Wahls, R.A., Morrison, J.H., Brodersen, O.P., Crippa, S., Mavriplis, D.J., and Murayama, M., "Summary of Dada from the Fifth AIAA CFD Drag Prediction Workshop", AIAA 2013-0046, January 2013.

[52] Raveh, D.E., "CFD-Based Models of Aerodynamic Gust Response", *Journal of Aircraft*, Vol. 44, No. 3, May-June 2007.

[53] Bartels, R.E., "Development, Verification and Use of Gust Modeling in the NASA Computational Fluid Dynamics Code FUN3D", NASA/TM-2012-217771, October 2012.

[54] Bartels, R.E., "Development of Accurate CFD Based Gust Model for the Truss Braced Wing Aircraft", AIAA 2013-3044, June 2013.

[55] Reimer, L., Ritter, M., Heinrich, R., and Krueger, W., "CFD-based Gust Load Analysis of a Free-flying flexible Passenger Aircraft in Comparison to a DLM-Based Approach", AIAA 2015-2455, June 2015.

[56] Frink, N.T., "Strategy for Dynamic CFD Simulations on SACCON Configuration", AIAA 2010-4559, June 2010.

[57] Salas, M.D., "Digital Flight: The Last CFD Aeronautical Grand Challenge", *Journal of Scientific Computing*, Vol. 28, No. 2/3, September 2006, pp. 479-505. doi: 10.1007/s10915-006-9087-7

[58] Meakin, R., Atwood, C., and Hariharan, N., "Development, Deployment, and Support of a Set of Multi-Disciplinary, Physics-Based Simulation Software Products," 49th AIAA Aerospace Sciences Meeting, Orlando,Florida, 4-7 January 2011.

[59] Morton, S.A. and McDaniel, D.R., "HPCMP CREATETM-AV Kestrel Current Capabilities and Future Direction for Fixed Wing Aircraft Simulations", AIAA 2015-0039, January 2015.

[60] Kroll, N., Abu-Zurayk, M., Dimitrov, D., Franz, T., Führer, T., Gerhold, T., Görtz, S., Heinrich, R., Ilic, C., Jepsen, J., Jägersküpper, J., Kruse, M., Krumbein A., Langer, S., Liu, D., Liepelt, R., Reimer, L., Ritter, M., Schwöppe, A., Scherer, J., Spiering, F., Thormann, R., Togiti, V., Vollmer, D., Wendisch, J.-H., "DLR-Projekt Digital-X – Auf dem Weg zur virtuellen Flugzeugentwicklung und Flugerprobung auf Basis höherwertiger Verfahren", DLRK2014-340099, Deutscher Luft- und Raumfahrtkongress 2014, Augsburg, 16–18. September 2014. Translated title: "Towards a virtual airplane development and flight testing based on higher-order methods"

[61] Forsythe, J.R., Lynch, C.E., Polsky, S., and Spalart, P., "Coupled Flight Simulator and CFD Calculations of Ship Airwake using HPCMP CREATE-AV Kestrel", AIAA 2015-0556, January 2015.

[62] Mukherjee, R. and Gopalarathnam, A., "Poststall Prediction of Multiple-Lifting-Surface Configurations Using a Decambering Approach", Journal of Aircraft, Vol. 43, No. 3, May-June 2006, pp. 660-668.

[63] Paul, R. C. and Gopalarathnam, A., "Iteration schemes for rapid post-stall aerodynamic prediction of wings using a decambering approach," *International Journal of Numerical Methods in Fluids*, Vol. 76, Issue 4, pages 199-222, October 2014. doi: 10.1002/fld.3931

[64] Paul, R. C., and Gopalarathnam, A., "Simulation of Flight Dynamics with an Improved Post-Stall Aerodynamics Model," AIAA Paper 2012-4956, August 2012.

[65] Paul, R. C., Murua, J., and Gopalarathnam, A., “Unsteady and Post-Stall Aerodynamic Modeling for Aircraft Dynamics Simulation,” IFASD-2015-070, International Forum on Aeroelasticity and Structural Dynamics, St. Petersburg, Russia, June 2015.

[66] Petrilli, J., Paul, R. C., Gopalarathnam, A., and Frink, N.T., "A CFD Database for Airfoils and Wings at Post-Stall Angles of Attack," AIAA Paper 2013-2916, June 2013.

[67] Harper, C. W. and Maki, R. L., “A Review of the Stall Characteristics of Swept Wings,” NASA TN D-2373, 1964.

[68] Hoerner, S. F., and Borst, H. V., *Fluid-Dynamic Lift*, Second Ed., Hoerner Fluid Dynamics, 1975.

[69] McLean, D., *Understanding Aerodynamics: Arguing from the Real Physics*, Chapter 8 (Lift and Wings in 3D at Subsonic Speeds), page 453, John Wiley & Sons, Ltd, Chichester, UK, 2012. doi: 10.1002/9781118454190.ch8

[70] Hosangadi, P., Paul, R. C., and Gopalarathnam, A., "Improved Stall Prediction for Swept Wings Using Low-Order Aerodynamics," AIAA Paper 2015-3159, June 2015.

[71] Klein, Vladislav, and Morelli, Eugene A., Aircraft System Identification Theory and Practice. AIAA Education Series, 2006.

[72] Murphy, P.C., Klein, V., Frink, Neal T., and Vicroy, Dan D., “System Identification Applied to Dynamic CFD Simulation and Wind-tunnel Data,” AIAA Atmospheric Flight Mechanics Conference, AIAA 2011-6522, August 2011.

[73] Murphy, P.C., Klein, V., “Estimation of Unsteady Aerodynamic Models from Dynamic Wind-tunnel Data”, NATO/RTO-MP-AVT-189, Chapter 20, October 2011.

[74] Murphy, P.C., Klein, V., and Frink, Neal T., “Unsteady Aerodynamic Modeling in Roll for the NASA Generic Transport Model”, AIAA 2012-4652, August 2012.

[75] Murphy, Patrick C., Klein, Vladislav, and Frink, Neal T., “Nonlinear Unsteady Aerodynamic Modeling Using Wind-tunnel and Computational Data,” to be published AIAA JGCD, 2016.

[76] Morelli, Eugene A., “Efficient Global Aerodynamic Modeling from Flight Data,” AIAA 2012-1050, January 2012.

[77] Dean, J.P., Morton, S.A., McDaniel, D.R., Clifton, J.D., and Bodkin, D.J., “Aircraft Stability and Control Characteristics by System Identification of CFD Simulations”, AIAA 2008-6378, August 2008.

[78] Ghoreyshi, M., and Cummings, R. M., “Unsteady Aerodynamics Modeling for Aircraft Maneuvers: A New Approach Using Time- Dependent Surrogate Modeling,” AIAA Paper 2012-3327, June 2012.

[79] Mackman, T.J., Allen, C.B., Ghoreyshi, M., and Badcock, K.J., “Comparison of Adaptive Sampling Methods for Generation of Surrogate Aerodynamic Models”, AIAA Journal, Vol. 51, No. 4, April 2013, doi: 10.2514/1.J051607

[80] Ghoreyshi, M., Cummings, R. M., Da Ronch, A., and Badcock, K. J., “Transonic Aerodynamic Load Modeling of X-31 Aircraft Pitching Motions,” *AIAA Journal*, Vol. 51, No. 10, 2013, pp. 2447–2464. doi: 10.2514/1.J052309

[81] Ghoreyshi, M., and Cummings, R. M., “Challenges in the Aerodynamics Modeling of an Oscillating and Translating Airfoil at Large Incidence Angles,” Aerospace Science and Technology, Vol. 28, No. 1, 2013, pp. 176–190. doi: 10.1016/j.ast.2012.10.013

[82] Ghoreyshi, M., and Cummings, R.M., “Unsteady Aerodynamic Modeling of Aircraft Control Surfaces by Indicial Response Methods”, *AIAA Journal*, Vol. 52, No. 12, December 2014, pp. 2683-2700. doi: 10.2514/1.J052946

[83] Ghoreyshi, M., Jirásek, A. and M. Cummings, R.M., “Reduced-Order Unsteady Aerodynamic Modeling for Stability and Control Analysis Using Computational Fluid Dynamics”, Progress in Aerospace Sciences 71 (2014) pp. 167-217.

[84] Strang, W.Z., Tomaro, R.F., and Grismer, J.J., “The Defining Methods of Cobalt: A Parallel, Implicit, Unstructured Euler/Navier-Stokes Flow Solver”, AIAA 1999-0786, January 1999.

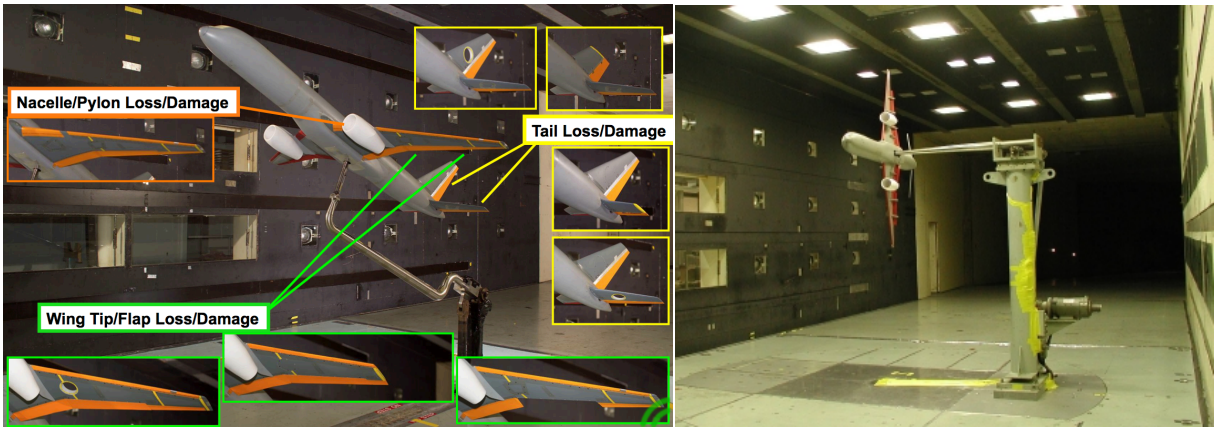

Figure 1. – Generic Transport Model (GTM) in NASA LaRC 14X22 Foot Subsonic Tunnel. Left - static mount with representative airframe damage. Right – pitch oscillation mount.

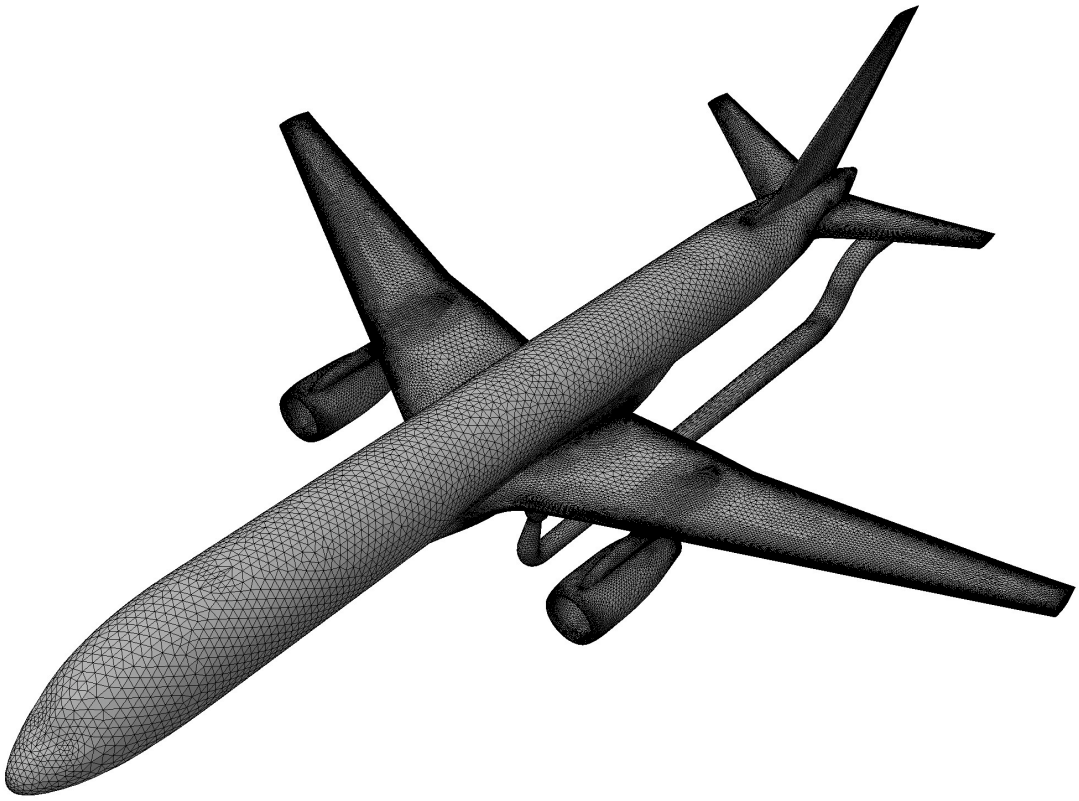

Figure 2. - Typical triangular surface grid on GTM.

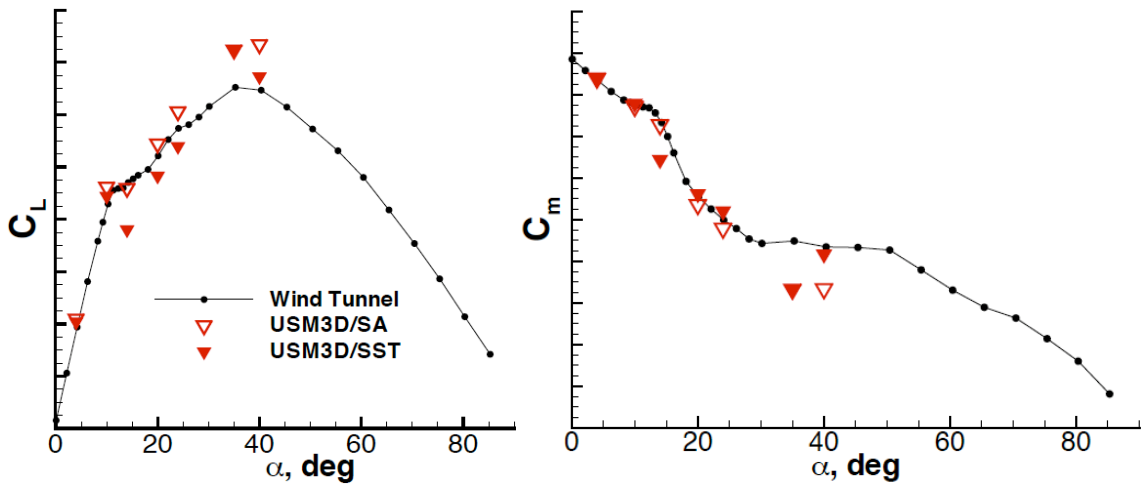

Figure 3. - Effect of turbulence model on static lift and pitching moment coefficient on 6-million half-span GTM grid. 14X22 WT M_{∞}=0.077, M_{USM3D}=0.2, Re_{cref}=0.54x10^6.

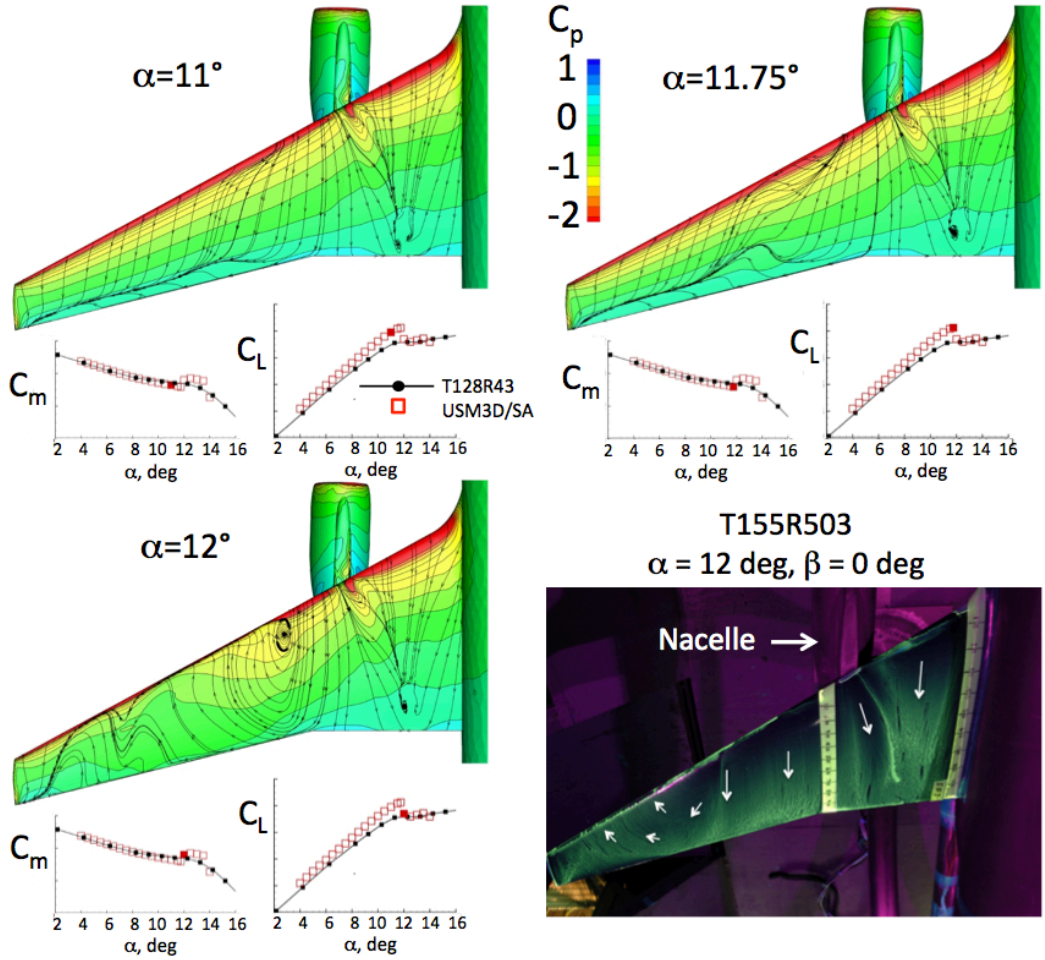

Figure 4. - Correlation of surface flows with lift and pitching moment and 12 Foot LWT oil flow through stall.

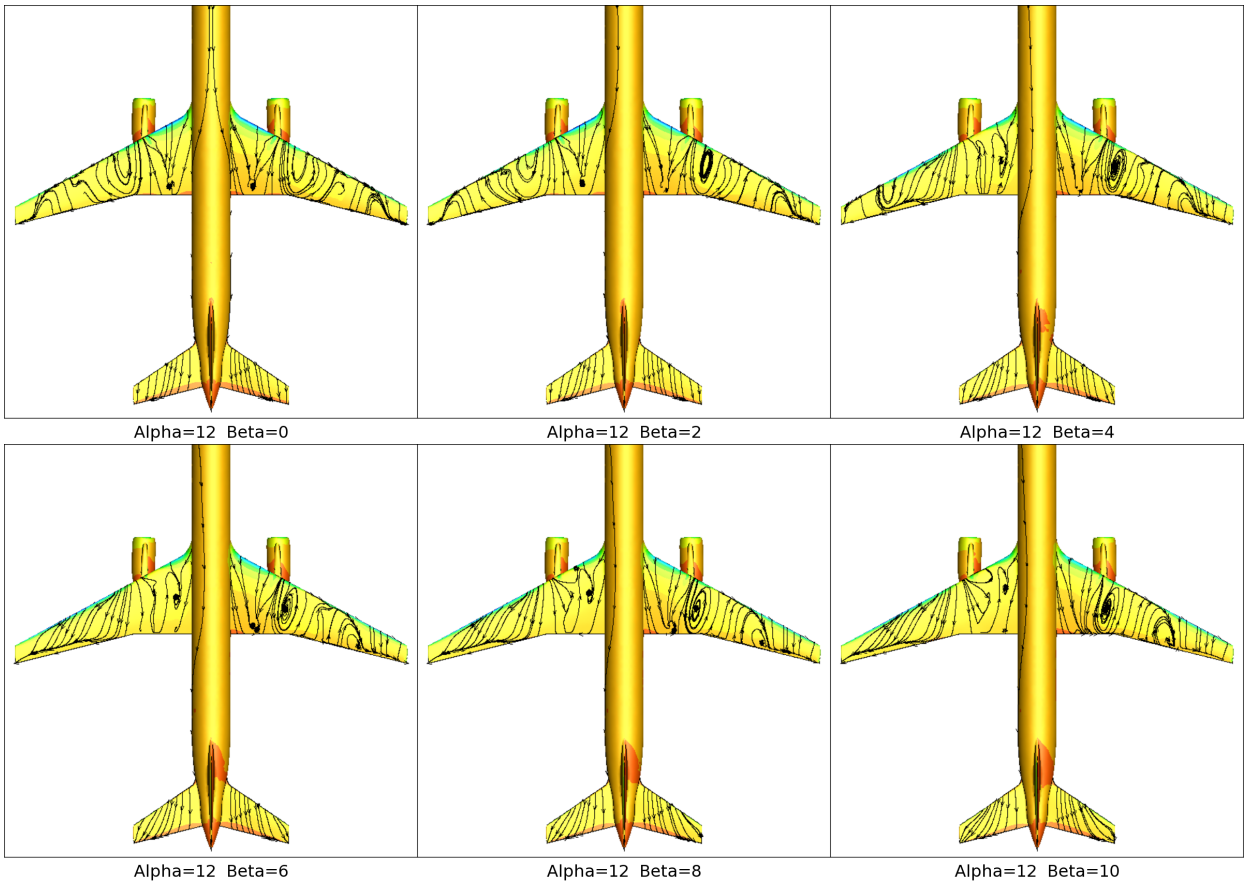

Figure 5. - Progression of GTM surface flow patterns with sideslip during stall. USM3D/SA. α=12°, M_∞=0.2, Re_{cref}=0.54x10^6.

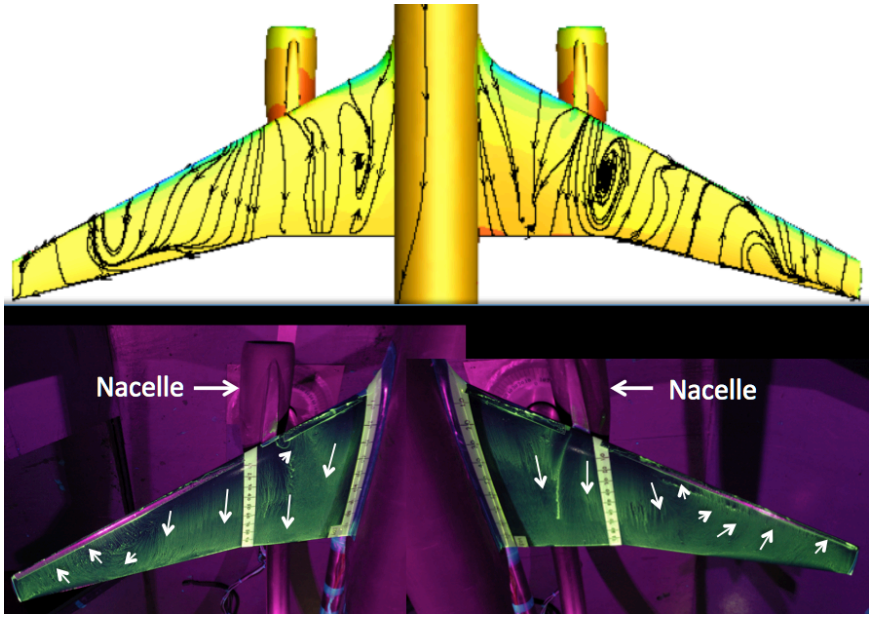

Figure 6. – Effect of sideslip on surface flow patterns of GTM at stall (α=12°, β=4°). USM3D/SA (top), 12 FT LWT T105/R103 (bottom).

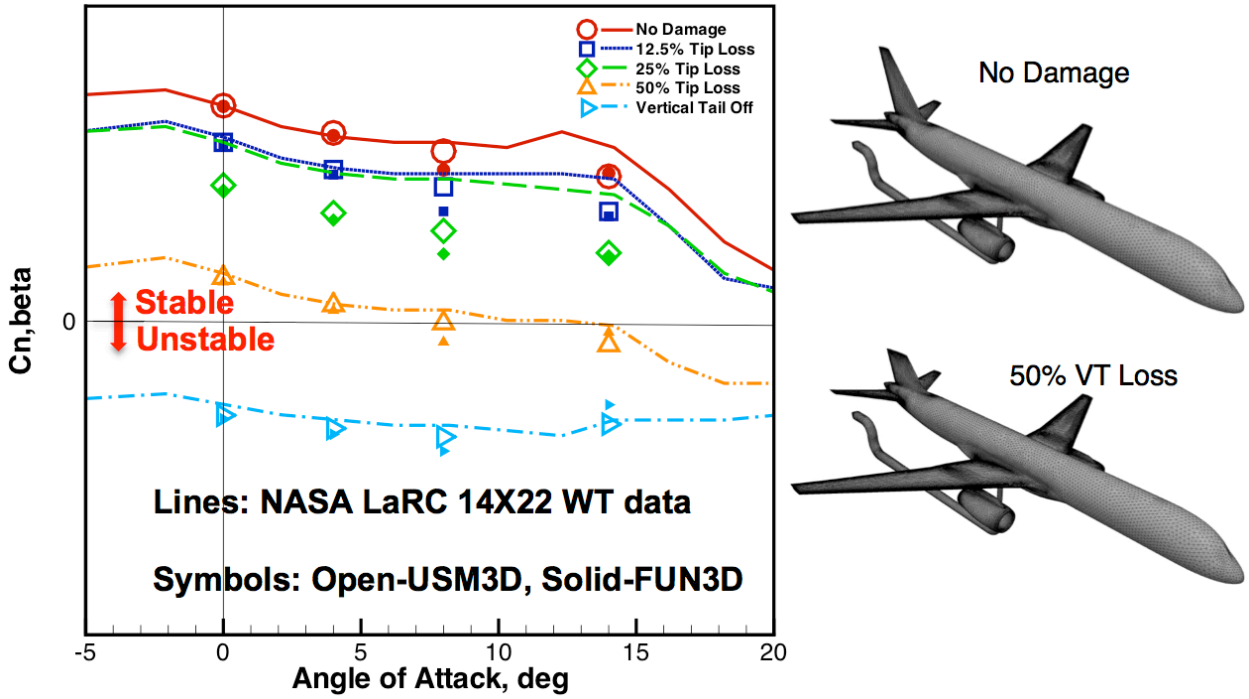

Figure 7. - Effect of vertical tail damage on static directional stability for GTM at β=0°.

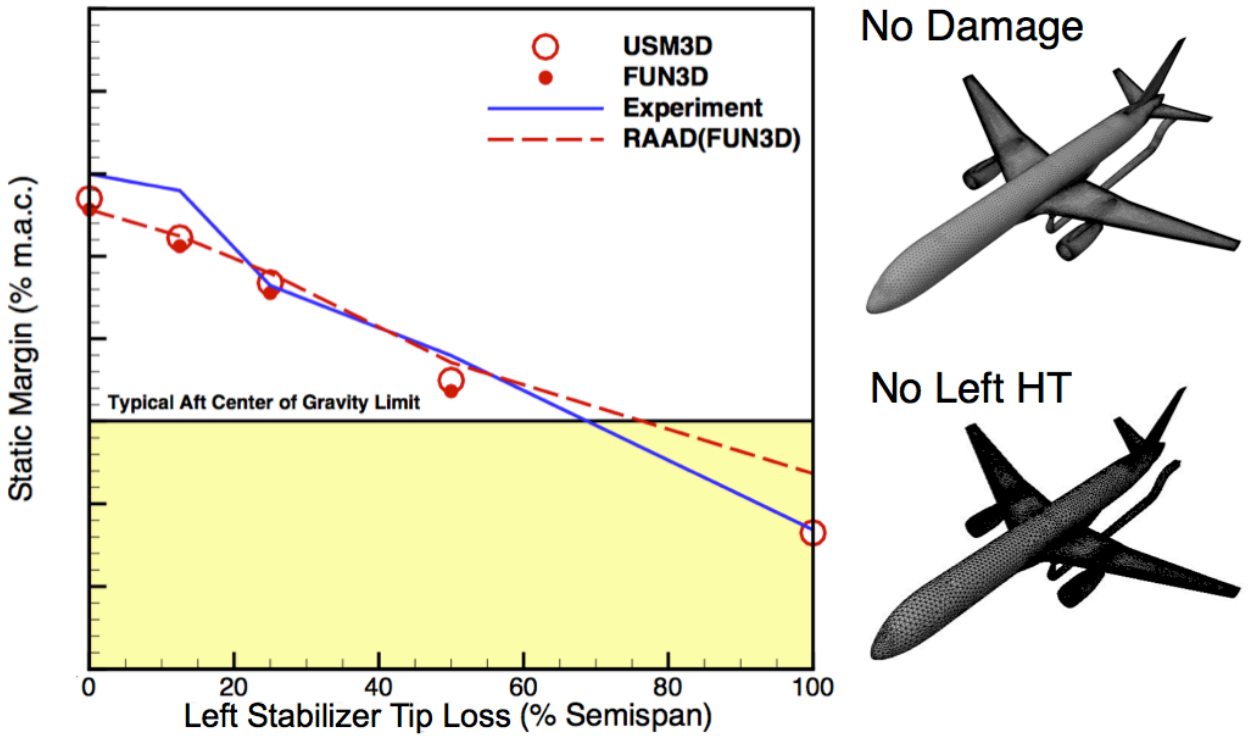

Figure 8. - Impact of left horizontal tail damage on static margin of GTM. β=0°.

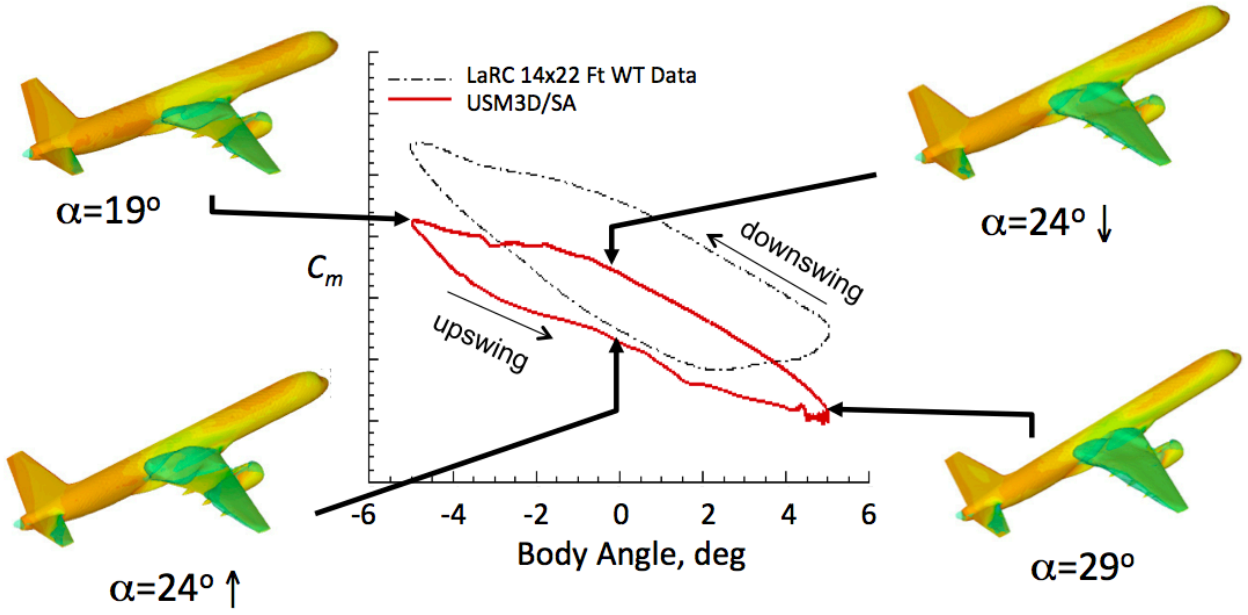

Figure 9. - Correlation of upper surface flow separation with hysteresis of C_m for GTM undergoing sinusoidal oscillation, $\Delta\alpha$=+/-5° about α_0=24°.

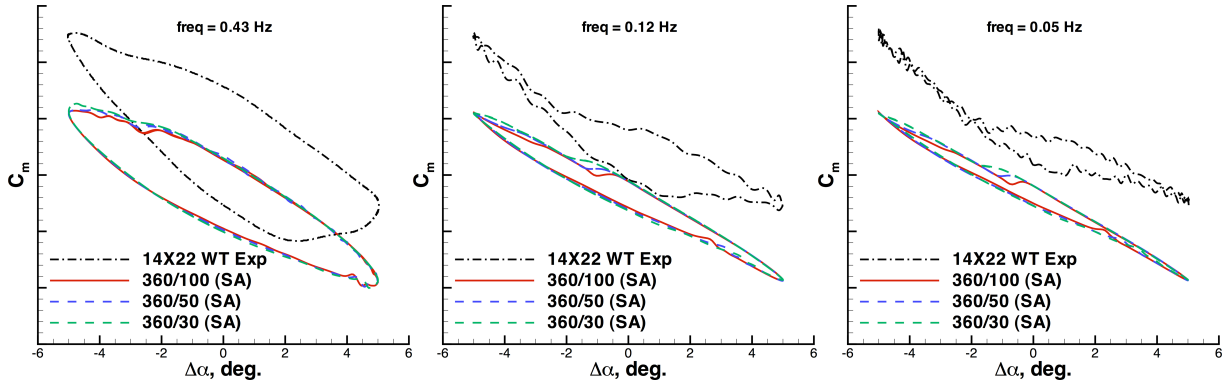

Figure 10. - Effect of subiteration on GTM with larger amplitude of pitch oscillation (a_0=24°, $\Delta\alpha$=+/-5°) using 360 time steps per cycle. 14X22 M_∞=0.08, USM3D/(SA and SST) M_{USM3D}=0.2, Re_{cref}=0.54x10^6, L-R: Frequencies a) 0.43 Hz, b) 0.12 Hz, and c) 0.05 Hz.

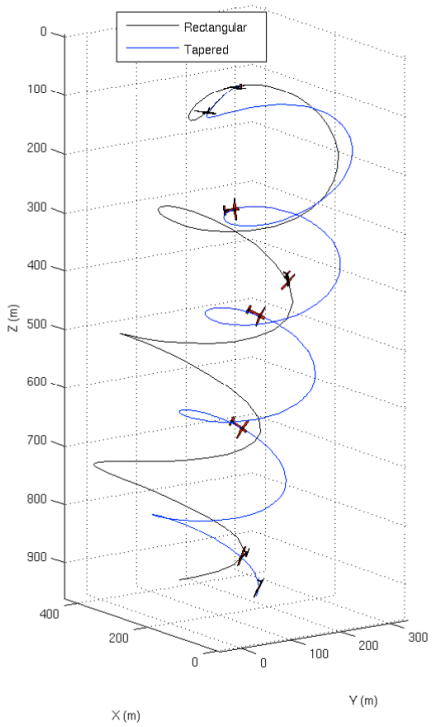

Figure 11. - Post-stall flight trajectories simulated using the decambering approach. Results are shown for the rectangular and tapered wing planform options.

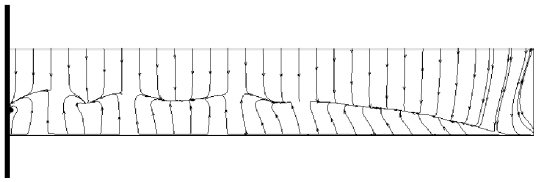

(a) Sweep=0 deg., α=18 deg.

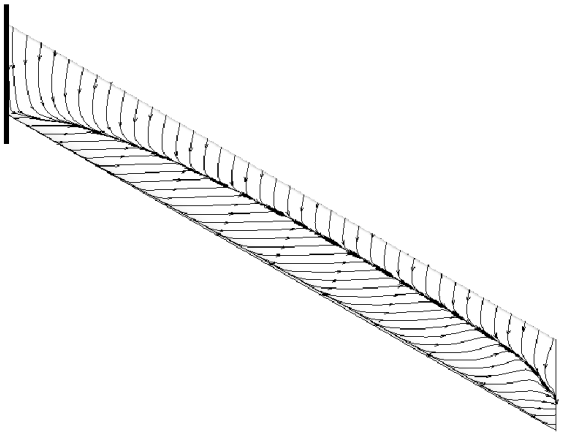

(b) Sweep=30 deg, α =18 deg

Figure 12. - Upper-surface skin-friction lines for AR-12 wing with NACA 4415 airfoil at $Re_{cref}=3x10^6$. USM3D/SA.

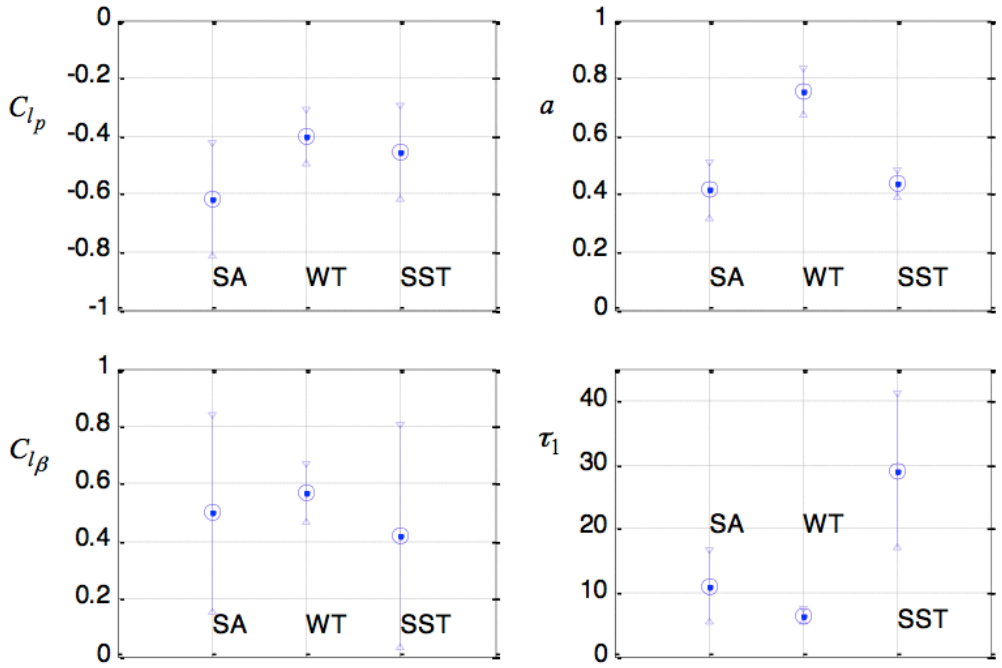

Figure 13. - SID model parameter estimates and 2σ error bounds at α=20°, using wind-tunnel (WT) and USM3D CFD roll oscillatory data on SACCON. Δϕ=+/-5°.

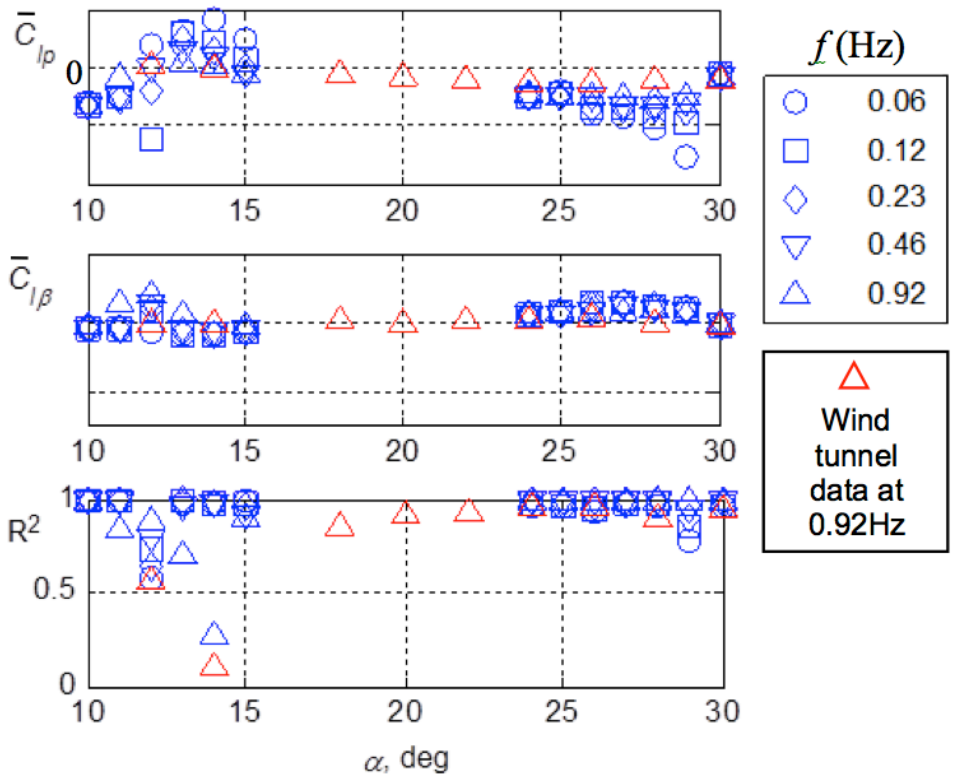

Figure 14. - Harmonic analysis of CFD simulated rolling moment coefficient on NASA GTM. USM3D/SA. Roll oscillations Δϕ=+/-20°.

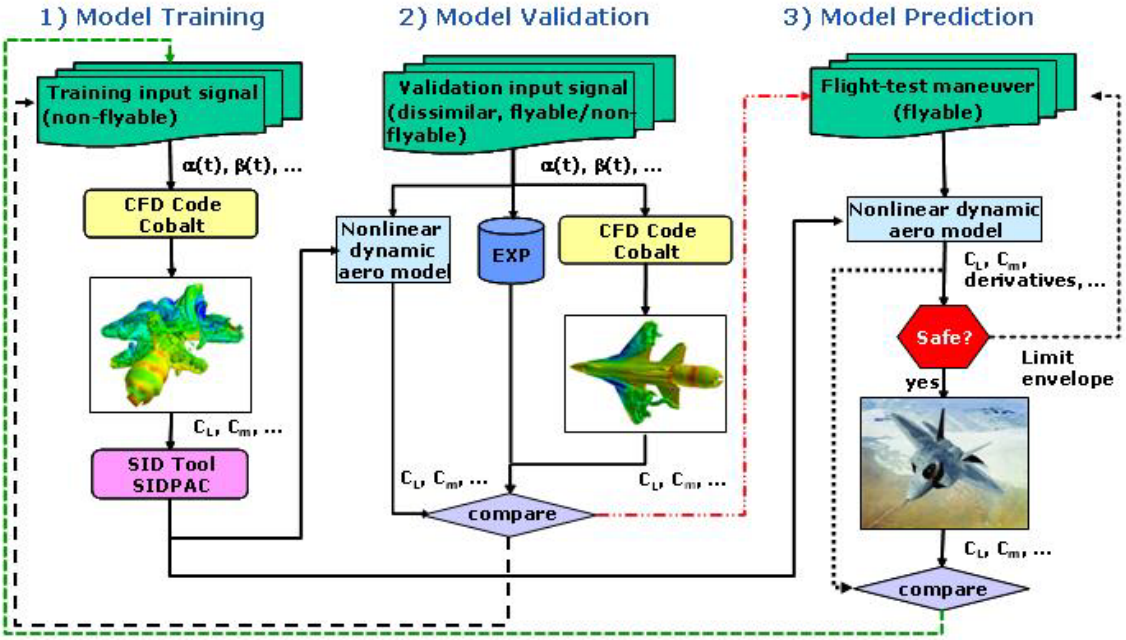

Figure 15. - AFSEO stability and control model build process [77].

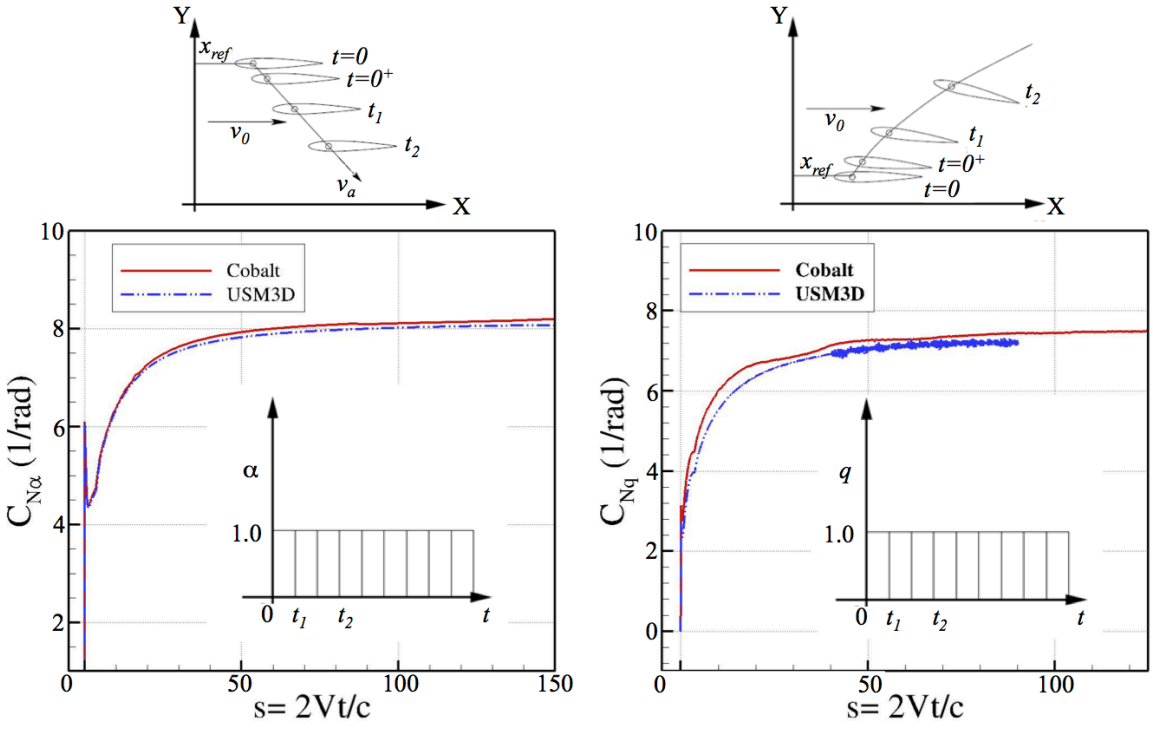

Figure 16. - NACA 0012 airfoil indicial responses of C_N to unit step changes in angle-of-attack and pitch rate from two CFD codes. Left - α_0=0°, Δα=1°, q=0. Right - α=0°, Δq=1 rad/sec. Mach=0.6. [32]

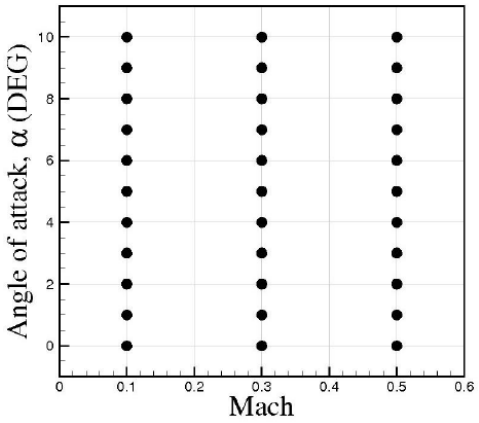

Figure 17. - Sample design space for nonlinear ROM. Maneuver constraints: $0.1 \leq M \leq 0.5$, $-10° \leq \alpha \leq 10°$ (assumes symmetry about $\alpha=0°$).

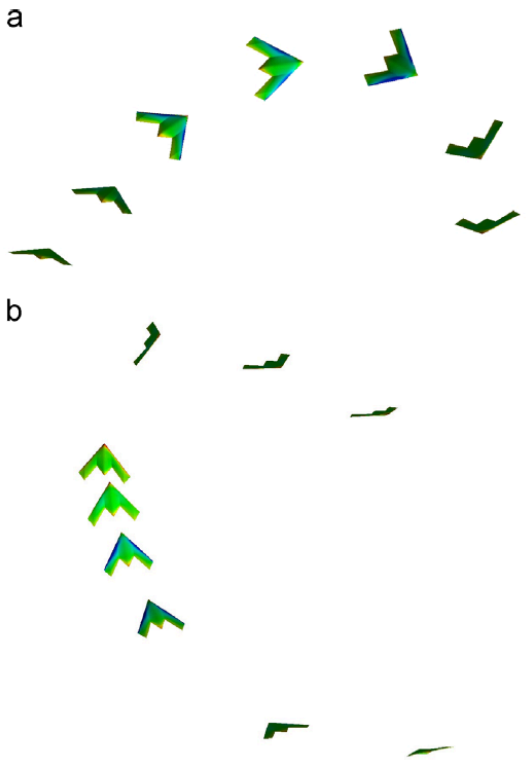

Figure 18. - *Cobalt* CFD surface pressure solutions on AVT-201 SACCON during flight maneuvers: (a) half Lazy-8 and (b) Immelmann turn. [78], [83]